

Auxiliary Cross-Modal Common Representation Learning with Triplet Loss Functions for Online Handwriting Recognition

Anonymous authors

Paper under double-blind review

Abstract

Common representation learning (CRL) learns a shared embedding between two or more modalities to improve in a given task over using only one of the modalities. CRL from different data types such as images and time-series data (e.g., audio or text data) requires a deep metric learning loss that minimizes the distance between the modality embeddings. In this paper, we propose to use the triplet loss, which uses positive and negative identities to create sample pairs with different labels, for CRL between image and time-series modalities. By adapting the triplet loss for CRL, higher accuracy in the main (time-series classification) task can be achieved by exploiting additional information of the auxiliary (image classification) task. Our experiments on synthetic data and handwriting recognition data from sensor-enhanced pens show an improved classification accuracy, faster convergence, and a better generalizability.

1 Introduction

Cross-modal retrieval such as common representation learning (CRL) Peng et al. (2017) for learning across two or more modalities (i.e., image, audio, text and 3D data) has attracted a lot of attention recently. It can be applied in a wide range of applications such as multimedia management Lee et al. (2020) and identification Sarafianos et al. (2019). Extracting information from several modalities and adapting the domain with cross-modal learning allows to use information in all domains Ranjan et al. (2015). CRL, however, remains challenging due to the *heterogeneity gap* (inconsistent representation forms of different modalities) Huang et al. (2020).

A limitation of CRL is that most approaches require the availability of all modalities at inference time. However, in many applications certain data sources are only available during training by means of elaborate laboratory setups Lim et al. (2019). For instance, consider a human pose estimation task that uses inertial sensors together with RGB videos during training. A camera setup might not be available at inference time due to bad lighting conditions or other application-specific restrictions. This requires a model that allows inference on the main modality only, while auxiliary modalities may only be used to improve the training process (as they are not available at inference time) Hafner et al. (2022). *Learning using privileged information* Vapnik & Izmailov (2015) is one approach in the literature that describes and tackles this problem. During training it is assumed that in addition to X additional information X^* , the *privileged information*, is available which is, however, not present in the inference stage Momeni & Tatwawadi (2018).

For CRL, we need a deep metric learning (DML) technique that aims to transform training samples into feature embeddings that are close for samples that belong to the same class and far apart for samples from different classes Wei et al. (2016). As DML requires no model update (simply fine-tuning for training samples of new classes), DML is an interesting approach for continual learning Do et al. (2019). Typical DML methods use simple distances (e.g., Euclidean distance) but also highly complex distances (e.g., canonical correlation analysis Ranjan et al. (2015) and maximum mean discrepancy Long et al. (2015)). While CRL learns representations from all modalities, single-modal learning commonly uses pair-wise learning. The triplet loss Schroff et al. (2015) selects a positive and negative triplet pair for a corresponding anchor and forces the positive pair distance to be smaller than the negative pair distance.

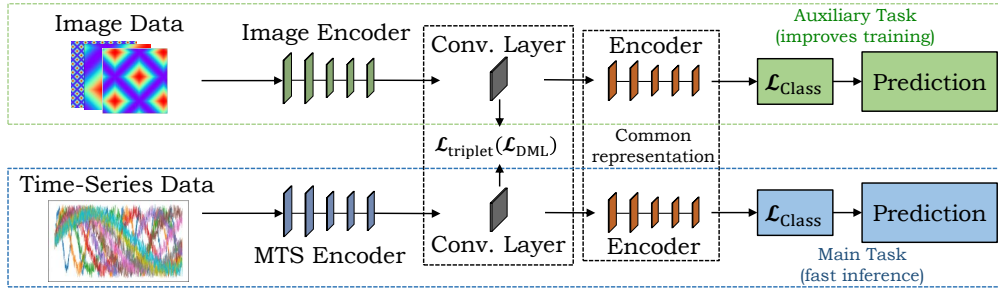


Figure 1: **Method overview:** Common representation learning between image and time-series data using the triplet loss based on DML functions to improve the time-series classification task.

While research of triplet selection for single-modal classification is very advanced Do et al. (2019), pair-wise selection for CRL is investigated for specific applications only Zhen et al. (2015); Lee et al. (2020); Zhang & Zheng (2020).

One exemplary application for cross-modal learning is handwriting recognition (HWR). HWR can be categorized into offline and online HWR. Offline HWR such as optical character recognition (OCR) deals with the analysis of the visual representation of handwriting only, but cannot be applied for real-time recognition applications Fahmy (2010). Online HWR works on different types of spatio-temporal signals and can make use of temporal information such as writing speed and direction Plamondon & Srihari (2000). Many recording systems make use of a stylus pen together with a touch screen surface Alimoglu & Alpaydin (1997). Systems for writing on paper are only prototypical Chen et al. (2021); Schrapel et al. (2018); Wang et al. (2013); Deselaers et al. (2015) and cannot be applied for real-world applications. A novel sensor-enhanced pen based on inertial measurement units (IMUs) enables new applications for writing on normal paper. This pen has previously been used for single character Ott et al. (2020; 2022a;b) and sequence Ott et al. (2022c) classification. However, the accuracy of previous online HWR methods is limited due to the limited size of datasets as recording of larger amounts of data is time consuming. A possible solution is to combine datasets of different modalities using common representation learning to increase the generalizability. In this work, we combine offline HWR from generated images (i.e., OCR) and online HWR from sensor-enhanced pens by learning a common representation between both modalities. The aim is to integrate information of OCR, i.e., typeface, cursive or printed writing, and font thickness, into the online HWR task, i.e., writing speed and direction Vinciarelli & Perrone (2003).

Our Contribution. Models that use rich data (e.g., images) usually outperform those that use a less rich modality (e.g., time-series). We therefore propose to train a shared representation using the triplet loss between pairs of image and time-series data to learn a common representation between both modality embeddings (cf. Figure 1). This allows to improve the accuracy for single-modal inference in the main task. We prove the efficacy of our DML-based triplet loss for CRL both with simulated data and in a real-world application. More specifically, our proposed CRL technique 1) improves the multivariate time-series (MTS) classification accuracy and convergence, 2) results in a small MTS-only network independent from the image modality while allowing for fast inference, and 3) has better generalizability and adaptability Huang et al. (2020). Code and datasets are available upon publication.¹

The paper is organized as follows. Section 2 discusses related work followed by the mathematical foundation of our method in Section 3. The experimental setup is described in Section 4 and the results are discussed in Section 5.

2 Related Work

In this section, we discuss related work, in particular approaches for learning a common representation from different modalities (in Section 2.1) and DML (in Section 2.2) to minimize the distance between feature embeddings.

2.1 Cross-Modal Representation Learning

For traditional methods that learn a common representation, a cross-modal similarity for the retrieval can be calculated with linear projections as basic models Rasiwasia et al. (2010). However, cross-modal correlation is highly complex,

¹Code and datasets: <https://www.anonymous-submission.org>

and hence, recent methods are based on a *modal-sharing network* to jointly transfer non-linear knowledge from a single modality to all modalities Wei et al. (2016). Huang et al. (2020) use a *cross-modal network* between different modalities (image to video, text, audio and 3D models) and a *single-modal network* (shared features between images of source and target domains). They use two convolutional layers (similar to our proposed architecture) that allows the model to adapt more trainable parameters. However, while their auxiliary network uses the same modality, our auxiliary network is based on another modality. Lee et al. (2020) learn a common embedding between video frames and audio signals with graph clusters, but at inference both modalities must be available. Sarafianos et al. (2019) proposed an image-text modality adversarial matching approach that learns modality-invariant feature representations, but their projection loss is used for learning discriminative image-text embeddings only. Hafner et al. (2022) propose a model for single-modal inference. However, they use image and depth modalities for person re-identification without a time-series component, which makes the problem considerably different. Lim et al. (2019) handled multisensory modalities for 3D models only.

2.2 Deep Metric Learning

Networks trained for the classification task can produce useful feature embeddings with efficient runtime complexity $\mathcal{O}(NC)$ per epoch, where N is the number of training samples and C the number of classes. The classical cross-entropy (CE) loss, however, is not useful for DML as it ignores how close each point is to its class centroid (or how far apart from other class centroids). The *pairwise contrastive loss* Chopra et al. (2005) minimizes the distance between feature embedding pairs of the same class and maximizes the distance between feature embedding pairs of different classes dependent on a margin parameter. The issue is that the optimization of positive pairs is independent from negative pairs, but the optimization should force the distance between positive pairs to be smaller than negative pairs Do et al. (2019).

The *triplet loss* Yoshida et al. (2019) addresses this by defining an anchor and a positive as well as a negative point, and forces the positive pair distance to be smaller than the negative pair distance by a certain margin. The runtime complexity of the triplet loss is $\mathcal{O}(N^3/C)$, and can be computationally challenging for large training sets. Hence, several works exist to reduce this complexity such as hard or semi-hard triplet mining Schroff et al. (2015), or smart triplet mining Harwood et al. (2017). Often, data is evolving over time, and hence, Semedo & Magalhães (2020) proposed a formulation of the triplet loss where the traditional static *margin* is superseded by a temporally adaptive maximum margin function. While Zeng et al. (2017); Li et al. (2021) combine the triplet loss with the CE loss, Guo et al. (2019) use a triplet selection with L_2 -normalization for language modeling, but considered all negative pairs for triplet selection with fixed similarity intensity parameter. For our experiments, we use a triplet loss with a dynamic margin together with a novel word level triplet selection. The DeepTripletNN Zeng et al. (2020) also uses the triplet loss on embeddings between an anchor from audio data and positive and negative samples from visual data, and the cosine similarity for the final representation comparison. CrossATNet Chaudhuri et al. (2020), another triplet loss-based method which uses single class labels, defines class sketch instances as anchor, the same class image instance as positive sample and a different class image instance as negative sample. While the previous methods are based on a triplet selection method using single label classification, we are – to the best of our knowledge – the first to propose the triplet loss for sequence-based classification (i.e., words).

Most of the related work uses the Euclidean metric as distance loss, although the triplet loss can be defined based on any other (sub-)differentiable distance metric. Wan & Zou (2021) proposed a method for offline signature verification based on a dual triplet loss that uses the Euclidean space to project an input image to an embedding function. While Rantzsche et al. (2016) use the Euclidean metric to learn the distance between feature embeddings, Zeng et al. (2017) use the Cosine similarity. Hermans et al. (2017) state that using the *non-squared* Euclidean distance is more stable, while the *squared* distance made the optimization more prone to collapsing. Recent methods extend the canonical correlation analysis (CCA) Ranjan et al. (2015) that learns linear projection matrices by maximizing pairwise correlation of cross-modal data. To share information between the same modality (i.e., images), typically the maximum mean discrepancy (MMD) Long et al. (2015) is minimized.

3 Methodology

We define the problem of common representation learning and present DML loss functions in Section 3.1. In Section 3.2 we propose the triplet loss for cross-modal learning.

3.1 Common Representation Learning

A multivariate time-series (MTS) $\mathbf{U} = \{\mathbf{u}_1, \dots, \mathbf{u}_m\} \in \mathbb{R}^{m \times l}$ is an ordered sequence of $l \in \mathbb{N}$ streams with $\mathbf{u}_i = (u_{i,1}, \dots, u_{i,l}), i \in \{1, \dots, m\}$, where $m \in \mathbb{N}$ is the length of the time-series. The MTS training set is a subset of the array $\mathcal{U} = \{\mathbf{U}_1, \dots, \mathbf{U}_{n_U}\} \in \mathbb{R}^{n_U \times m \times l}$, where n_U is the number of time-series. Let $\mathbf{X} \in \mathbb{R}^{o \times p}$ with entries $x_{i,j} \in [0, 255]$ represent an image from the image training set. The image training set is a subset of the array $\mathcal{X} = \{\mathbf{X}_1, \dots, \mathbf{X}_{n_X}\} \in \mathbb{R}^{n_X \times o \times p}$, where n_X is the number of time-series. The aim of joint MTS and image classification tasks is to predict an unknown class label $v \in \Omega$ for single class prediction or $\mathbf{v} \in \Omega$ for sequence prediction for a given MTS or image (see also Section 4.2). The time-series samples denote the main training data, while the image samples represent the privileged information that is not used for inference. In addition to good prediction performance, the goal is to learn representative embeddings $f_c(\mathbf{U})$ and $f_c(\mathbf{X}) \in \mathbb{R}^{q \times w}$ to map MTS and image data into a feature space $\mathbb{R}^{q \times w}$, where f_c is the output of the convolutional layer(s) $c \in \mathbb{N}$ of the latent representation.

We force the embedding to live on the $q \times w$ -dimensional hypersphere by using a Softmax attention, i.e., $\|f_c(\mathbf{U})\|_2 = 1$ and $\|f_c(\mathbf{X})\|_2 = 1 \forall c$ (see (Weinberger et al., 2005)). In order to obtain a small distance between the embeddings $f_c(\mathbf{U})$ and $f_c(\mathbf{X})$, we minimize DML functions $\mathcal{L}_{\text{DML}}(f_c(\mathbf{X}), f_c(\mathbf{U}))$. Well-known DML metrics are the distance-based mean squared error (MSE) \mathcal{L}_{MSE} , the spatio-temporal cosine similarity (CS) \mathcal{L}_{CS} , the Pearson correlation (PC) \mathcal{L}_{PC} , or the distribution-based Kullback-Leibler (KL) divergence \mathcal{L}_{KL} . In our experiments, we additionally evaluate the kernalized maximum mean discrepancy (kMMD) $\mathcal{L}_{\text{kMMD}}$, Bray Curtis (BC) \mathcal{L}_{BC} , and Poisson \mathcal{L}_{PO} losses. We study their performance in Section 5. A combination of classification and CRL losses can be realized by dynamic weight averaging Liu et al. (2019) as a multi-task learning approach that performs dynamic task weighting over time (see Appendix A.1).

3.2 Triplet Loss

While the training with the previous loss functions uses inputs where the image and MTS have the same label, pairs with similar but different labels can improve the training process. This can be achieved using the triplet loss Schroff et al. (2015) which enforces a margin between pairs of image and MTS data with the same identity to all other different identities. As a consequence, the convolutional output for one and the same label lives on a manifold, while still enforcing the distance and thus discriminability to other identities. We therefore seek to ensure that the embedding of the MTS \mathbf{U}_i^a (*anchor*) of a specific label is closer to the embedding of the image \mathbf{X}_i^p (*positive*) of the same label than it is to the embedding of any image \mathbf{X}_i^n (*negative*) of another label (see Figure 2). Thus, we want the following inequality to hold for all training samples $(f_c(\mathbf{U}_i^a), f_c(\mathbf{X}_i^p), f_c(\mathbf{X}_i^n)) \in \Phi$:

$$\mathcal{L}_{\text{DML}}(f_c(\mathbf{U}_i^a), f_c(\mathbf{X}_i^p)) + \alpha < \mathcal{L}_{\text{DML}}(f_c(\mathbf{U}_i^a), f_c(\mathbf{X}_i^n)), \quad (1)$$

where $\mathcal{L}_{\text{DML}}(f_c(\mathbf{X}), f_c(\mathbf{U}))$ is a DML loss, α is a margin between positive and negative pairs, and Φ is the set of all possible triplets in the training set. Based on (1), we can formulate a differentiable loss function that we can use for optimization:

$$\mathcal{L}_{\text{trpl},c}(\mathbf{U}^a, \mathbf{X}^p, \mathbf{X}^n) = \sum_{i=1}^N \max \left[\mathcal{L}_{\text{DML}}(f_c(\mathbf{U}_i^a), f_c(\mathbf{X}_i^p)) - \mathcal{L}_{\text{DML}}(f_c(\mathbf{U}_i^a), f_c(\mathbf{X}_i^n)) + \alpha, 0 \right], \quad (2)$$

where $c \in \mathbb{N}$.² Selecting negative samples that are too close to the anchor (in relation to the positive sample) can cause slow training convergence. Hence, triplet selection must be handled carefully and application-specific Do et al. (2019). We choose negative samples based on the class distance (single labels) and on the Edit distance (sequence labels), see Section 4.2.

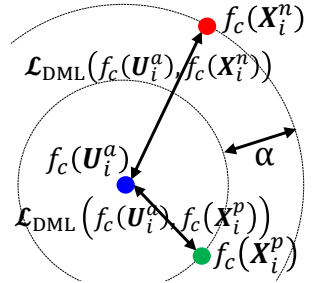


Figure 2: Triplet pair.

²To have a larger number of trainable parameters in the latent representation with a greater depth, we evaluate one and two stacked convolutional layers, each trained with a shared loss $\mathcal{L}_{\text{trpl},c}$.

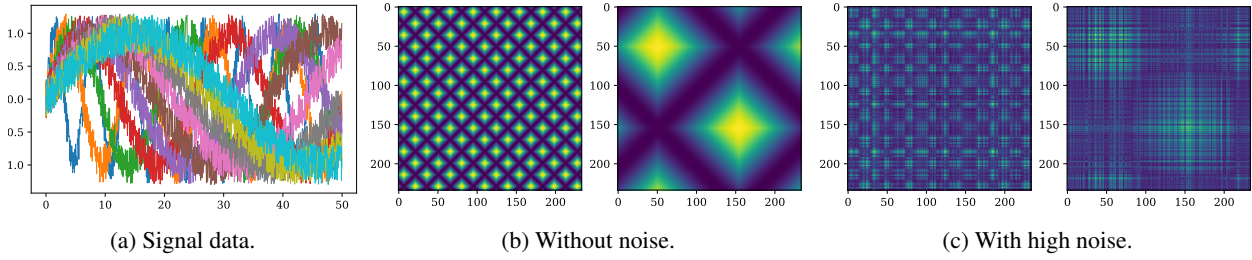


Figure 3: Synthetic signal data (a) for 10 classes, and image data (b-c) for classes 0 (left) and 6 (right).

4 Experiments

We now demonstrate the efficacy of our proposal. In Section 4.1 we generate sinusoidal time-series with introduced noise (main task) and compute the corresponding Gramian angular summation field (GASF) with different noise parameters (auxiliary task), see Figure 1. In Section 4.2 we combine online (inertial sensor signals, main task) and offline data (visual representations, auxiliary task) for handwriting recognition (HWR) with sensor-enhanced pens. This task is particularly challenging due to different data representations based on images and MTS data. For both applications, our approach allows to only use the main modality (MTS) for inference. We further analyze and evaluate different DML functions to minimize the distance between the learned embeddings.

4.1 Cross-Modal Learning on Synthetic Data

We first investigate the influence of the triplet loss for cross-modal learning between synthetic time-series and image-based data. For this, we generate signal data of 1,000 timesteps with different frequencies for 10 classes (see Figure 3a) and add noise from a continuous uniform distribution $U(a, b)$ for $a = 0$ and $b = 0.3$. We use a recurrent CNN with the CE loss to classify these signals. From each signal without noise, we generate a GASF Wang & Oates (2015). For classes with high frequencies, this results in a fine-grained pattern, and for low frequencies in a coarse-grained pattern. We generate GASFs with different added noise between $b = 0$ (Figure 3b) and $b = 1.95$ (Figure 3c). A small CNN classifies these images with the CE loss. To combine both networks, we train each signal-image pair with the triplet loss. As the frequency of the sinusoidal signal is closer for more similar class labels, the distance in the manifold embedding should also be closer. For each batch, we select negative sample pairs for samples with the class label $CL = 1 + \lfloor \frac{\max_e - e - 1}{25} \rfloor$ as lower bound for current epoch e and maximum epoch \max_e . We set the margin α in the triplet loss separately for each batch such that $\alpha = \beta \cdot (CL_p - CL_n)$ depends on the positive CL_p and negative CL_n class labels of the batch and is in the range $[1, 5]$ with $\beta = 0.1$. The batch size is 100 and $\max_e = 100$. Appendix A.2 provides further details. This combination of the CE loss with the triplet loss can lead to a mutual improvement of the utilization of the classification task and embedding learning.

4.2 Cross-Modal Learning for HWR

Method Overview. Figure 4 gives a method overview. The main task is online HWR to classify words written with a sensor-enhanced pen and represented by MTS of the different pen sensors. To improve the classification task with a better generalizability, the auxiliary network performs offline HWR based on an image input. We pre-train ScrabbleGAN Fogel et al. (2020) on the IAM-OffDB Liwicki & Bunke (2005) dataset and for all MTS word labels generate the corresponding image as the positive MTS-image pair. Each MTS and each image is associated with \mathbf{v} , a sequence of L class labels from a pre-defined label set Ω with K classes. For our classification task, $\mathbf{v} \in \Omega^L$ describes words. The MTS training set is a subset of the array \mathcal{U} with labels $\mathcal{V}_U = \{\mathbf{v}_1, \dots, \mathbf{v}_{n_U}\} \in \Omega^{n_U \times L}$. The image training set is a subset of the array \mathcal{X} , and the corresponding labels $\mathcal{V}_X = \{\mathbf{v}_1, \dots, \mathbf{v}_{n_X}\} \in \Omega^{n_X \times L}$. Offline HWR techniques are based on Inception, ResNet34, or GTR Yousef et al. (2018) modules. The online method is improved by sharing layers with a common representation by minimizing the distance of the feature embedding of the convolutional layers $c \in \{1, 2\}$ (integrated in both networks) with a shared loss $\mathcal{L}_{\text{shared}, c}$. We set the embedding size $\mathbb{R}^{q \times w}$ to 400×200 . Both networks are trained with the connectionist temporal classification (CTC) Graves

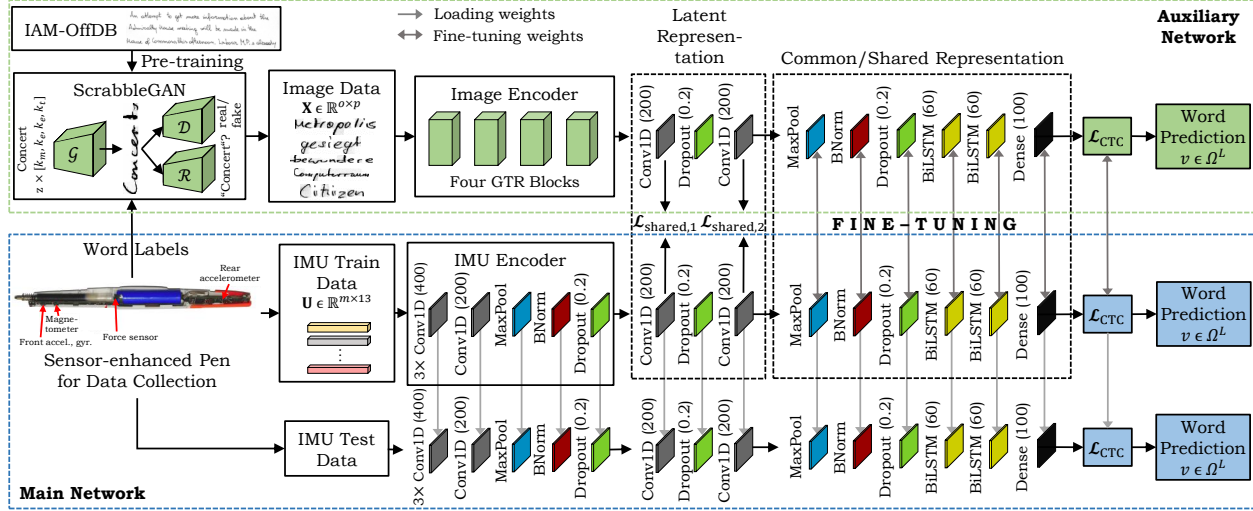


Figure 4: **Detailed method overview:** The middle pipeline consists of data recording with a sensor-enhanced pen, feature extraction of inertial MTS data, and word classification with CTC. We generate image data with the pre-trained ScrabbleGAN for corresponding word labels. The top pipeline (four GTR blocks) extracts features from images. The distances of the embeddings are minimized with the triplet loss and DML functions. The classification network with two BiLSTM layers are fine-tuned for the OnHW task for a common representation.

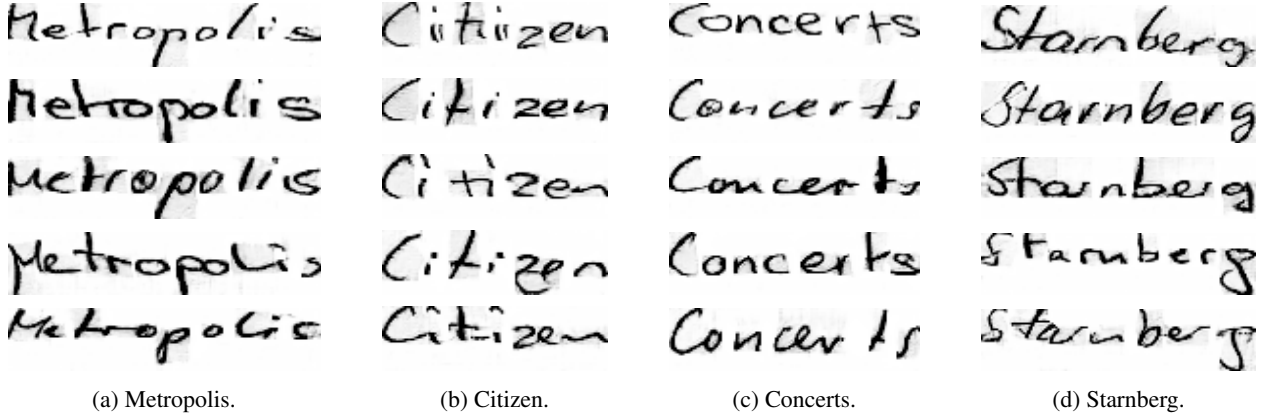


Figure 5: Overview of four generated words with ScrabbleGAN Fogel et al. (2020) with various text styles.

et al. (2009) loss \mathcal{L}_{CTC} to avoid pre-segmentation of the training samples by transforming the network outputs into a conditional probability distribution over label sequences.

Datasets for Online HWR. We make use of two word datasets proposed in Ott et al. (2022c). These datasets are recorded with a sensor-enhanced pen that uses two accelerometers (3 axes each), one gyroscope (3 axes), one magnetometer (3 axes), and one force sensor at 100 Hz Ott et al. (2020; 2022b). One sample of size $m \times l$ represents an MTS of a written word of m timesteps from $l = 13$ sensor channels. One word is a sequence of small or capital characters (52 classes) or with mutated vowels (59 classes). The *OnHW-words500* dataset contains 25,218 samples where each of the 53 writers contributed the same 500 words. The *OnHW-wordsRandom* dataset contains 14,641 randomly selected words from 54 writers. For both datasets, 80/20 train/validation splits are available for writer-independent (WD/WI) tasks. We transform (zero padding, interpolation) all samples to 800 timesteps.

Image Generation for Offline HWR. In order to couple the online MTS data with offline image data, we use a generative adversarial network (GAN) to generate arbitrarily many images. ScrabbleGAN Fogel et al. (2020) is a state-of-the-art semi-supervised approach that consists of a generator \mathcal{G} that generates images of words with arbitrary length

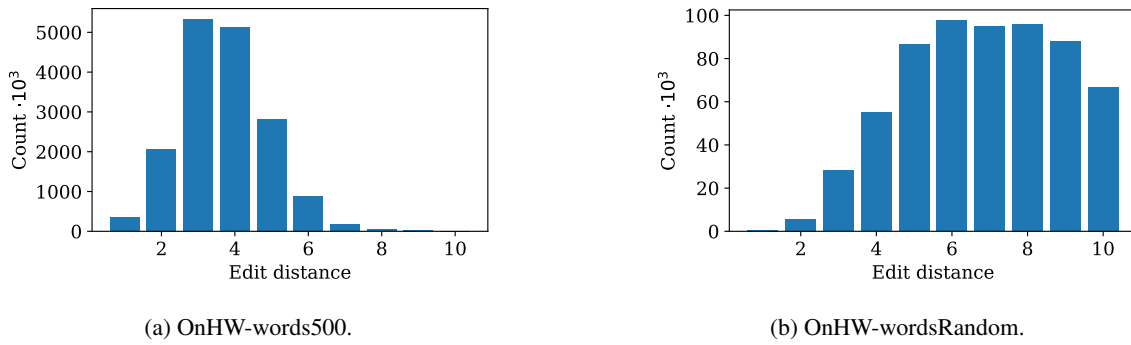


Figure 6: Number image-MTS pairs dependent on mismatches.

from an input word label, a discriminator \mathcal{D} , and a recognizer \mathcal{R} promoting style and data fidelity. For the generator, four character filters (k_m , k_e , k_e and k_t) are concatenated, multiplied by a noise vector and fed into a class-conditioned generator. This allows for adjacent characters to interact, e.g., enabling cursive text. We train ScrabbleGAN with the IAM-OffDB Liwicki & Bunke (2005) dataset and generate three different datasets. Exemplary images are shown in Figure 5. First, we generate 2 million images randomly selected from a large lexicon (*OffHW-German*), and pre-train the offline HWR architectures. Second, we generate 100,000 images based on the same word labels for each of the OnHW-words500 and OnHW-wordsRandom datasets (*OffHW-[words500, wordsRandom]*), and fine-tune the offline HWR architectures.

Methods for Offline HWR. OrigamiNet Yousef & Bishop (2020) is a state-of-the-art multi-line recognition method using only unsegmented image and text pairs. An overview of offline HWR methods is given in Appendix A.3. Similar to OrigamiNet, our offline method is based on different encoder architectures with one or two additional 1D convolutional layers (each with filter size 200, Softmax activation Zeng et al. (2017)) with 20% dropout for the latent representation, and a common representation decoder with BiLSTMs. For the encoder, we make use of Inception modules from GoogLeNet, the ResNet34 architecture, and re-implement the newly proposed gated, fully convolutional method gated text recognizer (GTR) Yousef et al. (2018). See Appendix A.4 for detailed information on the architectures. We train the networks on the generated OffHW-German dataset for 10 epochs, and fine-tune on the OffHW-[500, wordsRandom] datasets for 15 epochs. For comparison with state-of-the-art techniques, we train OrigamiNet and compare with IAM-OffDB. For OrigamiNet, we apply interline spacing reduction via seam carving Avidan & Shamir (2007), resizing the images to 50% height, and random projective (rotating and resizing lines) and random elastic transform Wigington et al. (2017). We augment the OffHW-German dataset with random width resizing and apply no augmentation for the OffHW-[words500, wordsRandom] datasets for fine-tuning.

Offline/Online Common Representation Learning. Our architecture for online HWR is based on Ott et al. (2022c). The encoder extracts features of the inertial data and consists of three convolutional layers (each with filter size 400, ReLU activation) and one convolutional layer (filter size 200, ReLU activation), a max pooling, batch normalization and a 20% dropout layer. As for the offline architecture, the network then learns a latent representation with one or two convolutional layers (each with filter size 200, Softmax activation) with 20% dropout and the same CRL decoder. The output of the convolutional layers of the latent representation are minimized with the $\mathcal{L}_{\text{shared},c}$ loss. The layers of the common representation are fine-tuned based on the pre-trained weights of the offline technique. Here, two BiLSTM layers with 60 units each and ReLU activation extract the temporal context of the feature embedding. As for the baseline classifier, we train for 1,000 epochs. For evaluation, the main MTS network is independent of the image auxiliary network by using only the weights of the main network.

Triplet Selection. To ensure (fast) convergence, it is crucial to select triplets that violate the constraint from Equation 1. Typically, it is infeasible to compute the loss for all triplet pairs or this leads to poor training performance as poorly chosen pairs dominate hard ones. This requires an elaborate triplet selection Do et al. (2019). We use the Edit distance (ED) to define the identity and select triplets. The ED is the minimum number of substitutions S , insertions I and deletions D required to change the sequences $\mathbf{h} = (h_1, \dots, h_r)$ into $\mathbf{g} = (g_1, \dots, g_t)$ with length r and t , respec-

tively. We define two sequences with an ED of 0 as positive pair, and with an ED larger than 0 as negative pair. Based on preliminary experiments, we use only substitutions for triplet selection that lead to a higher accuracy compared to additional insertions and deletions (whereas these would also change the length difference of image and MTS pairs). We constrain $p - m/2$, the difference in pixels p of the images and half the number of timesteps of the MTS, to be maximal ± 20 . The goal is a small distance for positive pairs, and a large distance for negative pairs that increases with a larger ED (between 1 and 10). And despite a limited number of word labels, there still exist a large number of image-MTS pairs per word label for every possible ED (see Figure 6). For each batch, we search in a dictionary of negative sample pairs for samples with $ED = 1 + \lfloor \frac{\max_e - e - 1}{100} \rfloor$ as lower bound for the current epoch e and maximal epochs \max_e . For every label we randomly pick one image. We let the margin α in the triplet loss vary for each batch such that $\alpha = \beta \cdot \overline{ED}$ is depending on the mean ED of the batch and is in the range $[1, 11]$ with $\beta = 10^{-3}$ for MSE, $\beta = 0.1$ for CS and PC, and $\beta = 1$ for KL. The batch size is 100 and $\max_e = 1,000$.

5 Experimental Results

Hardware and Training Setup. For all experiments we use Nvidia Tesla V100-SXM2 GPUs with 32 GB VRAM equipped with Core Xeon CPUs and 192 GB RAM. We use the vanilla Adam optimizer with a learning rate of 10^{-4} .

5.1 Evaluation of Synthetic Data

We train the time-series (TS) model 18 times with noise $b = 0.3$, and the combined model with the triplet loss for all 40 noise combinations ($b \in \{0, \dots, 1.95\}$) with different DML functions. Figure 7 shows the validation accuracy averaged over all trainings as well as the combined cases separately for noise $b < 0.2$ and noise $0.2 \leq b < 2.0$ (for the \mathcal{L}_{CS} loss). The accuracy of the models that use only images and in combination with MTS during inference reach an accuracy of 99.7% (which can be seen as an unreachable upper bound for the TS-only models). The triplet loss improves the final TS baseline accuracy from 92.5% to 95.36% (averaged over all combinations) while combining TS and image data leads to a faster convergence. Conceptually similar to Long et al. (2015), we use the \mathcal{L}_{KMMMD} loss which yields 95.83% accuracy. The \mathcal{L}_{PC} (96.03%), \mathcal{L}_{KL} (96.22%), \mathcal{L}_{MSE} (96.25%), \mathcal{L}_{BC} (96.62%), and \mathcal{L}_{PO} (96.76%) loss functions can further improve the accuracy. We conclude that the triplet loss can be successfully used for cross-modal learning by utilizing negative identities.

5.2 Evaluation of HWR

Evaluation Metrics. A metric for sequence evaluation is the character error rate (CER) defined as $CER = \frac{S_c + I_c + D_c}{N_c}$ as the Edit distance (the sum of character substitutions S_c , insertions I_c and deletions D_c) divided by the total number of characters in the set N_c . Similarly, the word error rate (WER) is defined as $WER = \frac{S_w + I_w + D_w}{N_w}$ computed with word operations S_w , I_w and D_w , and number of words in the set N_w .

Evaluation of Offline HWR Methods. All our models yield low error rates on the generated OffHW-German dataset. Our approach with GTR blocks outperforms (0.24% to 0.44% CER) the models with Inception (1.27% CER) and ResNet (1.24% CER). OrigamiNet achieves the lowest error rates of 1.50% WER and 0.11% CER. Four GTR blocks yield the best results at a significantly lower training time compared to six or eight blocks. We fine-tune the model with four GTR blocks for one and two convolutional layers and achieve notably low error rates between 0.22% to 0.76% CER, and between 0.85% to 2.95% WER on the OffHW-[words500, wordsRandom] datasets. For more results, see Appendix A.5.

Evaluation of CRL Feature Embeddings. Table 1 shows the feature embeddings for image $f_2(\mathbf{X}_i)$ and MTS data $f_2(\mathbf{U}_i)$ of the *positive* sample Export and the two *negative* samples Expert ($ED = 1$) and Import ($ED = 2$) based on four DML loss functions. The pattern of characters are similar as the words differ only in the fourth letter.

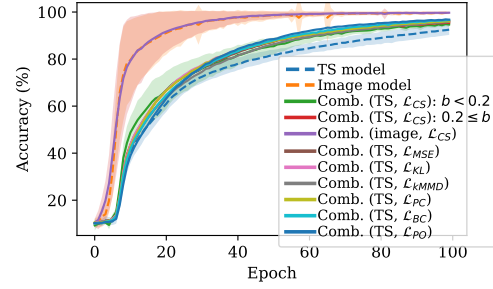
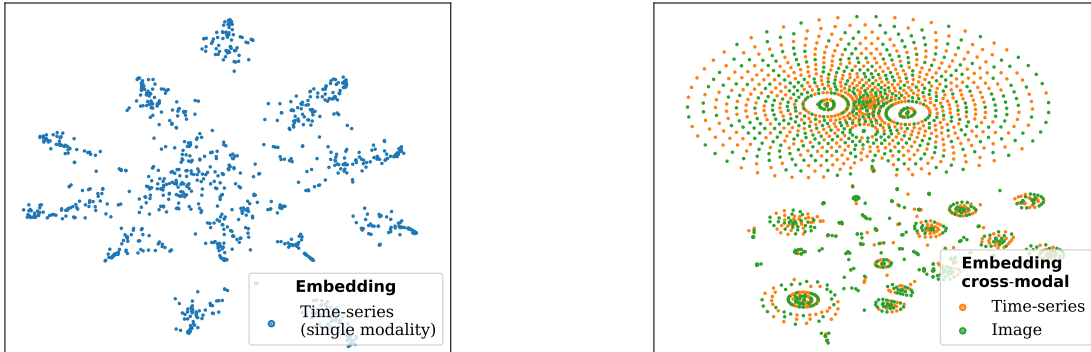


Figure 7: Comparison of single- and cross-modal CRL.

Table 1: Feature embeddings $f_c(\mathbf{X}_i)$ and $f_c(\mathbf{U}_i)$ of exemplary image \mathbf{X}_i and MTS \mathbf{U}_i data of the convolutional layer $c = \text{conv}_2$ for different deep metric learning functions for positive pairs ($ED = 0$) and negative pairs ($ED > 0$) trained with the triplet loss. The feature embeddings are similar in the red box (character x) or blue box (character p) for $f_2(\mathbf{X}_i)$, or the last pixels (character t) of $f_2(\mathbf{U}_i)$ for \mathcal{L}_{PC} marked green.

ED	Label	Image \mathbf{U}_i	$f_2(\mathbf{X}_i)$	$f_2(\mathbf{U}_i): \mathcal{L}_{\text{MSE}}$	$f_2(\mathbf{U}_i): \mathcal{L}_{\text{CS}}$	$f_2(\mathbf{U}_i): \mathcal{L}_{\text{PC}}$	$f_2(\mathbf{U}_i): \mathcal{L}_{\text{KL}}$
0	Export	<i>expor L</i>					
		<i>Expert</i>					
1	Expert	<i>Import</i>					
		<i>Vorort</i>					
2	Import						
3	Vorort						



(a) Feature embedding of IMU samples for the single modality

(b) Feature embeddings of IMU and image samples for the cross-modal network.

Figure 8: Plot of 400×200 feature embeddings of image and IMU modalities with t-SNE.

In contrast, **Import** has a different feature embedding as the replacement of E with I and x with m leads to a higher feature distance in the embedding hypersphere. Note that image and MTS data can vary in length for $ED > 0$. Figure 8 shows the feature embeddings of the output of the convolutional layers ($c = 1$) processed with t-SNE van der Maaten & Hinton (2008). Figure 8a visualizes the MTS embeddings $f_1(\mathbf{U}_i)$ of the single modal network, and Figure 8b visualizes the MTS and image embeddings, $f_1(\mathbf{U}_i)$ and $f_1(\mathbf{X}_i)$ respectively, in a cross-modal setup. While the embedding of the single modal network is unstructured, the embeddings of the cross-modal network are structured (distance of samples visualizes the Edit distance between words).

Evaluation of Cross-Modal CRL. Table 2 gives an overview of CRL (for $c = 1$). The first row are baseline results by Ott et al. (2022c): 13.04% CER on OnHW-words500 (WD) and 6.75% CER on OnHW-wordsRandom (WD) with mutated vowels (MV). Compared to various time-series classification techniques, their benchmark results showed superior performance of CNN+BiLSTMs on these OnHW recognition tasks. In general, the word error rate (WER) can vary for a similar character error rate (CER). The reason is that a change of one character of a correctly classified

Table 2: Evaluation results (WER and CER in %) average over five splits of the baseline MTS-only technique and our cross-modal learning technique for the inertial-based OnHW datasets Ott et al. (2022c) with and without mutated vowels (MV) for one convolutional layer $c = 1$.

Method	OnHW-words500				OnHW-wordsRandom			
	WD		WI		WD		WI	
	WER	CER	WER	CER	WER	CER	WER	CER
\mathcal{L}_{CTC} , w/ MV	42.81	13.04	60.47	28.30	37.13	6.75	83.28	35.90
\mathcal{L}_{CTC} , w/o MV	42.77	13.44	59.82	28.54	38.02	7.81	83.54	36.51
\mathcal{L}_{MSE}	40.76	12.71	55.54	25.97	37.31	7.01	82.25	33.85
\mathcal{L}_{CS}	38.62	11.55	56.37	25.90	38.85	7.35	82.48	35.67
\mathcal{L}_{PC}	39.09	11.69	57.90	27.23	38.46	7.15	82.71	35.13
\mathcal{L}_{KL}	38.36	11.28	60.23	27.99	38.76	7.49	81.07	33.96
$\mathcal{L}_{\text{trpl},1}(\mathcal{L}_{\text{MSE}})$	42.95	14.13	56.48	26.66	37.66	7.04	81.64	34.39
$\mathcal{L}_{\text{trpl},1}(\mathcal{L}_{\text{CS}})$	38.01	11.29	58.50	27.10	37.12	6.98	82.71	33.09
$\mathcal{L}_{\text{trpl},1}(\mathcal{L}_{\text{PC}})$	40.43	12.41	58.20	27.48	37.40	7.01	81.90	33.89
$\mathcal{L}_{\text{trpl},1}(\mathcal{L}_{\text{KL}})$	37.55	11.21	63.52	30.52	38.39	7.36	83.18	35.21

word leads to a large change in the WER, while the change of the CER is marginal. We compare to results without MV as ScrabbleGAN is pretrained on IAM-OffDB that does not contain MV, and hence, such words cannot be generated. Here, the error rates are slightly higher for both datasets. As expected, cross-modal learning improves the baseline results up to 11.28% CER on the OnHW-words500 WD dataset and up to 7.01% CER on the OnHW-wordsRandom WD dataset. With triplet loss, \mathcal{L}_{CS} outperforms other metrics on the OnHW-wordsRandom dataset, but is inconsistent on the OnHW-words500 dataset. The importance of the triplet loss is more significant for one convolutional layer ($c = 1$) than for two convolutional layers ($c = 2$), see Appendix A.5. Further, training with kMMD (implemented as in (Long et al., 2015)) does not yield reasonable results. We assume that this metric cannot make use of the important time component in the HWR application.

6 Conclusion

We evaluated DML-based triplet loss functions for CRL between image and time-series modalities with class label specific triplet selection. On synthetic data as well as on different HWR datasets, our method yields notable accuracy improvements for the main time-series classification task and can be decoupled from the auxiliary image classification task at inference time. Our cross-modal triplet selection further yields a faster training convergence with better generalization on the main task.

Broader Impact Statement

While research for offline handwriting recognition (HWR) is very advanced (an overview is proposed in the appendix), research for online HWR from sensor-enhanced only emerged in 2019. Hence, the methodological research currently does not meet the requirements for real-world applications. Handwriting is still important in different fields, in particular graphomotoric. The visual feedback provided by the pen helps young students to learn a new language. A well-known bottleneck for many machine learning algorithms is their requirement for large amounts of datasets, while data recording of handwriting data is time consuming. This paper extends the online HWR dataset with generated images from offline handwriting, and closes the gap between offline and online HWR by using offline HWR as auxiliary task by learning with privileged information. One downside of training the offline architecture (consisting of GTR blocks) is its long training time. But as this model is not required at inference time, processing the time-series is still fast. The common representation between both modalities (image and time-series) is achieved by using the triplet loss and a sample selection depending on the Edit distance. This approach is important in future applications of sequence-based classification as the triplet loss may also evolve for language processing applications as strong as in typically applied fields such as image recognition. Ethical statement about collection consent and personal information: For data recording, the consent of all participants was collected. The datasets only contain the raw data from the sensor-enhanced pen, and for statistics the age and gender of the participants and their handedness. The dataset is

fully pseudonymized by assigning an ID to every participant. The dataset does not contain any offensive content. The approach proposed in this paper, in particular used for the application of online handwriting recognition from sensor-enhanced pens, does not (1) facilitate injury to living beings, (2) raise safety or security concerns due to the anonymity of the data, (3) raise human rights concerns, (4) have a detrimental effect on people's livelihood, (5) develop harmful forms of surveillance as the data is pseudonymized, (6) damage the environment, and (7) deceive people in ways that cause harm.

References

- Fevzi Alimoglu and Ethem Alpaydin. Combining Multiple Representations and Classifiers for Pen-based Handwritten Digit Recognition. In *Intl. Conf. on Document Analysis and Recognition (ICDAR)*, volume 2, Ulm, Germany, August 1997.
- Shai Avidan and Ariel Shamir. Seam Carving for Content-Aware Image Resizing. In *ACM Trans. on Graphics (SIGGRAPH)*, volume 26(3), pp. 10, July 2007.
- Ushasi Chaudhuri, Biplab Banerjee, Avik Bhattacharya, and Mihai Datcu. CrossATNet - A Novel Cross-Attention based Framework for Sketch-based Image Retrieval. In *Image and Vision Computing*, volume 104, December 2020.
- Junshen Kevin Chen, Wanze Xie, and Yutong (Kelly) He. Motion-based Handwriting Recognition. In *arXiv preprint arXiv:2101.06022*, January 2021.
- Sumit Chopra, Raia Hadsell, and Yann LeCun. Learning a Similarity Metric Discriminatively, with Application to Face Verification. In *Intl. Conf. on Computer Vision and Pattern Recognition (CVPR)*, San Diego, CA, June 2005.
- Thomas Deselaers, Daniel Keysers, Jan Hosang, and Henry A. Rowley. GyroPen: Gyroscopes for Pen-Input with Mobile Phones. In *Trans. on Human-Machine Systems*, volume 45(2), pp. 263–271, January 2015.
- Thanh-Toan Do, Toan Tran, Ian Reid, Vijay Kumar, Tuan Hoang, and Gustavo Carneiro. A Theoretically Sound Upper Bound on the Triplet Loss for Improving the Efficiency of Deep Distance Metric Learning. In *Intl. Conf. on Computer Vision and Pattern Recognition (CVPR)*, pp. 10404–10413, Long Beach, CA, June 2019.
- Maged M. M. Fahmy. Online Signature Verification and Handwriting Classification. In *Journal on Ain Shams Engineering (ASEJ)*, volume 1(1), pp. 59–70, 2010.
- Sharon Fogel, Hadar Averbuch-Elor, Sarel Cohen, Shai Mazor, and Roee Litman. ScrabbleGAN: Semi-Supervised Varying Length Handwritten Text Generation. In *Intl. Conf. on Computer Vision and Pattern Recognition (CVPR)*, pp. 4324–4333, June 2020.
- Alex Graves, Marcus Liwicki, Santiago Fernández, Roman Bertolami, Horst Bunke, and Jürgen Schmidhuber. A Novel Connectionist System for Unconstrained Handwriting Recognition. In *Trans. on Pattern Analysis and Machine Intelligence (TPAMI)*, volume 31(5), pp. 855–868, May 2009.
- Dan Guo, Shengeng Tang, and Meng Wang. Connectionist Temporal Modeling of Video and Language: A Joint Model for Translation and Sign Labeling. In *Intl. Joint Conf. on Artificial Intelligence (IJCAI)*, pp. 751–757, 2019.
- Frank M. Hafner, Amran Bhuyian, Julian F. P. Kooij, and Eric Granger. Cross-Modal Distillation for RGB-Depth Person Re-Identification. In *Computer Vision and Image Understanding (CVIU)*, volume 103352, January 2022.
- Ben Harwood, Vijay Kumar B.G., Gustavo Carneiro, Ian Reid, and Tom Drummond. Smart Mining for Deep Metric Learning. In *Intl. Conf. on Computer Vision (ICCV)*, Venice, Italy, October 2017.
- Alexander Hermans, Lucas Beyer, and Bastian Leibe. In Defence of the Triplet Loss for Person Re-Identification. In *arXiv preprint arXiv:1703.07737*, March 2017.
- Xin Huang, Yuxin Peng, and Mingkuan Yuan. MHTN: Modal-Adversarial Hybrid Transfer Network for Cross-Modal Retrieval. In *Trans. on Cybernetics*, volume 50(3), pp. 1047–1059, 2020.

- Hyodong Lee, Joonseok Lee, Joe Yue-Hei Ng, and Paul Natsev. Large Scale Video Representation Learning via Relational Graph Clustering. In *Intl. Conf. on Computer Vision and Pattern Recognition (CVPR)*, Seattle, WA, June 2020.
- Wenbin Li, Xuesong Yang, Meihao Kong, Lei Wang, Jing Huo, Yang Gao, and Jiebo Luo. Triplet is All You Need with Random Mappings for Unsupervised Visual Representation Learning. In *arXiv preprint arXiv:2107.10419*, July 2021.
- Jae Hyun Lim, Pedro O. O. Pinheiro, Negar Rostamzadeh, Chris Pal, and Sungjin Ahn. Neural Multisensory Scene Inference. In *Advances in Neural Information Processing Systems (NIPS)*, volume 32, 2019.
- Shikun Liu, Edward Johns, and Andrew J. Davison. End-to-End Multi-Task Learning with Attention. In *Intl. Conf. on Computer Vision and Pattern Recognition (CVPR)*, pp. 1871–1880, Long Beach, CA, June 2019.
- Marcus Liwicki and Horst Bunke. IAM-OnDB - an On-Line English Sentence Database Acquired from Handwritten Text on a Whiteboard. In *Intl. Conf. on Document Analysis and Recognition (ICDAR)*, pp. 956–961, Seoul, Korea, August 2005.
- Mingsheng Long, Yue Cao, Lianmin Wang, and Michael I. Jordan. Learning Transferable Features with Deep Adaptation Networks. In *Intl. Conf. on Machine Learning (ICML)*, volume 37, pp. 97–105, July 2015.
- Ahmadreza Momeni and Kedar Tatwawadi. Understanding LUPI (Learning Using Privileged Information). 2018. URL <https://web.stanford.edu/~kedart/files/lUPI.pdf>.
- Felix Ott, Mohamad Wehbi, Tim Hamann, Jens Barth, Björn Eskofier, and Christopher Mutschler. The OnHW Dataset: Online Handwriting Recognition from IMU-Enhanced Ballpoint Pens with Machine Learning. In *Proc. of the ACM on Interactive, Mobile, Wearable and Ubiquitous Technologies (IMWUT)*, volume 4(3), article 92, Cancún, Mexico, September 2020.
- Felix Ott, David Rügamer, Lucas Heublein, Bernd Bischl, and Christopher Mutschler. Domain Adaptation for Time-Series Classification to Mitigate Covariate Shift. In *arXiv preprint arXiv:2204.03342*, April 2022a.
- Felix Ott, David Rügamer, Lucas Heublein, Bernd Bischl, and Christopher Mutschler. Joint Classification and Trajectory Regression of Online Handwriting using a Multi-Task Learning Approach. In *Proc. of the IEEE/CVF Winter Conf. on Applications of Computer Vision (WACV)*, pp. 266–276, Waikoloa, HI, January 2022b.
- Felix Ott, David Rügamer, Lucas Heublein, Tim Hamann, Jens Barth, Bernd Bischl, and Christopher Mutschler. Benchmarking Online Sequence-to-Sequence and Character-based Handwriting Recognition from IMU-Enhanced Pens. In *arXiv preprint arXiv:2202.07036*, February 2022c.
- Yuxin Peng, Xin Huang, and Yunzhen Zhao. An Overview of Cross-media Retrieval: Concepts, Methodologies, Benchmarks and Challenges. In *arXiv preprint arXiv:1704.02223*, April 2017.
- Rejean Plamondon and Sargur N. Srihari. On-line and Off-line Handwriting Recognition: A Comprehensive Survey. In *Trans. on Pattern Analysis and Machine Intelligence (TPAMI)*, volume 22(1), pp. 63–84, January 2000.
- Viresh Ranjan, Nikhil Rasiwasia, and C. V. Jawahar. Multi-Label Cross-Modal Retrieval. In *Intl. Conf. on Computer Vision (ICCV)*, Santiago de Chile, Chile, December 2015.
- Hannes Rantzs, Haojin Yang, and Christoph Meinel. Signature Embedding: Writer Independent Offline Signature Verification with Deep Metric Learning. In *Advances in Visual Computing (ISVC)*, pp. 616–625, December 2016.
- Nikhil Rasiwasia, Jose Costa Pereira, Emanuele Coviello, Gabriel Doyle, Gert R.G. Lanckriet, Roger Levy, and Nuno Vasconcelos. A New Approach to Cross-Modal Multimedia Retrieval. In *Intl. Conf. on Multimedia (MM)*, pp. 251–260, October 2010.
- Nikolaos Sarafianos, Xiang Xu, and Ioannis A. Kakadiaris. Adversarial Representation Learning for Text-to-Image Matching. In *Intl. Conf. on Computer Vision (ICCV)*, pp. 5814–5824, 2019.

- Maximilian Schrapel, Max-Ludwig Stadler, and Michael Rohs. Pentelligence: Combining Pen Tip Motion and Writing Sounds for Handwritten Digit Recognition. In *Conf. on Human Factors in Computing Systems*, number 131, pp. 1–11, April 2018.
- Florian Schroff, Dmitry Kalenichenko, and James Philbin. FaceNet: A Unified Embedding for Face Recognition and Clustering. In *arXiv preprint arXiv:1503.03832*, March 2015.
- David Semedo and João Magalhães. Adaptive Temporal Triplet-loss for Cross-modal Embedding Learning. In *ACM Intl. Conf. on Multimedia (MM)*, pp. 1152–1161, October 2020.
- Laurens van der Maaten and Geoffrey Hinton. Visualizing Data using t-SNE. In *Journal of Machine Learning Research (JMLR)*, volume 9(86), pp. 2579–2605, November 2008.
- Vladimir Vapnik and Rauf Izmailov. Learning Using Privileged Information: Similarity Control and Knowledge Transfer. In *Journal of Machine Learning Research (JMLR)*, pp. 2023–2049, September 2015.
- Alessandro Vinciarelli and Michael Peter Perrone. Combining Online and Offline Handwriting Recognition. In *Intl. Conf. on Document Analysis and Recognition (ICDAR)*, pp. 844–848, Edinburgh, UK, August 2003.
- Qian Wan and Qin Zou. Learning Metric Features for Writer-Independent Signature Verification using Dual Triplet Loss. In *Intl. Conf. on Pattern Recognition (ICPR)*, pp. 3853–3859, Milan, Italy, January 2021.
- Jeen-Shing Wang, Yu-Liang Hsu, and Cheng-Ling Chu. Online Handwriting Recognition Using an Accelerometer-Based Pen Device. In *Intl. Conf. on Computer Science and Engineering (CSE)*, 2013.
- Zhiguang Wang and Tim Oates. Imaging Time-Series to Improve Classification and Imputation. In *Intl. Joint. Conf. on Artificial Intelligence (IJCAI)*, pp. 3939–3945, Buenos Aires, Argentinia, July 2015.
- Yunchao Wei, Yao Zhao, Canyi Lu, Shikui Wei, Luoqi Liu, Zhenfeng Zhu, and Shuicheng Yan. Cross-Modal Retrieval with CNN Visual Features: A New Baseline. In *Trans. on Cybernetics*, volume 47(2), pp. 449–460, March 2016.
- Kilian Q. Weinberger, John Blitzer, and Lawrence K. Saul. Distance Metric Learning for Large Margin Nearest Neighbor Classification. In *Advances in Neural Information Processing Systems (NIPS)*, pp. 1473–1480, December 2005.
- Curtis Wigington, Seth Stewart, Brian Davis, Bill Barrett, Brian Price, and Scott Cohen. Data Augmentation for Recognition of Handwritten Words and Lines Using a CNN-LSTM Network. In *Intl. Conf. on Document Analysis and Recognition (ICDAR)*, Kyoto, Japan, November 2017.
- Tomoki Yoshida, Ichiro Takeuchi, and Masayuki Karasuyama. Safe Triplet Screening for Distance Metric Learning. In *Neural Computation*, volume 31(12), pp. 2432–2491, October 2019.
- Mohamed Yousef and Tom E. Bishop. OrigamiNet: Weakly-Supervised, Segmentation-Free, One-Step, Full Page Text Recognition by Learning to Unfold. In *Intl. Conf. on Computer Vision and Pattern Recognition (CVPR)*, pp. 14710–14719, Seattle, WA, June 2020.
- Mohamed Yousef, Khaled F. Hussain, and Usama S. Mohammed. Accurate, Data-Efficient, Unconstrained Text Recognition with Convolutional Neural Networks. In *arXiv preprint arXiv:1812.11894*, December 2018.
- Donghuo Zeng, Yi Yu, and Keizo Oyama. Deep Triplet Neural Networks with Cluster-CCA for Audio-Visual Cross-Modal Retrieval. In *ACM Trans. on Multimedia Computing, Communications, and Applications*, volume 16(3), pp. 1–23, August 2020.
- Xiangsheng Zeng, Donglai Xiang, Liangrui Peng, Changsong Liu, and Xiaoqing Ding. Local Discriminant Training and Global Optimization for Convolutional Neural Network Based Handwritten Chinese Character Recognition. In *Intl. Conf. on Document Analysis and Recognition (ICDAR)*, Kyoto, Japan, November 2017.
- Dawei Zhang and Zhonglong Zheng. Joint Representation Learning with Deep Quadruplet Network for Real-Time Visual Tracking. In *Intl. Conf. on Neural Networks (IJCNN)*, July 2020.
- Yi Zhen, Piyush Rai, Hongyuan Zha, and Lawrence Carin. Cross-Modal Similarity Learning via Pairs, Preferences, and Active Supervision. In *Association for the Advancement of Artificial Intelligence (AAAI)*, pp. 3203–3209, January 2015.

A Appendices

We present the multi-task learning technique in Section A.1, and show more details on learning with the triplet loss on synthetically generated signal and image data in Section A.2. We present an method overview for offline handwriting recognition (HWR) in Section A.3, and propose more details of our architectures in Section A.4. Section A.5 presents results of representation learning for HWR.

A.1 Multi-Task Learning (MTL)

We simultaneously train the \mathcal{L}_{CTC} loss for sequence classification combined with one or two shared losses $\mathcal{L}_{\text{shared},1}$ and $\mathcal{L}_{\text{shared},2}$ for common representation learning (CRL). As both losses are in different ranges, the naive weighting

$$\mathcal{L}_{\text{total}} = \sum_{i=1}^{|T|} \omega_i \mathcal{L}_i, \quad (3)$$

with pre-specified, constant weights $\omega_i = 1, \forall i \in \{1, \dots, |T|\}$ can harm the training process. Hence, we apply dynamic weight average (DWA) Liu et al. (2019) as an MTL approach that performs dynamic task weighting over time (i.e., after each batch).

A.2 Training Synthetic Data with the Triplet Loss

Signal and Image Generation. We combine the networks for both, signal and image classification, to improve the classification accuracy over each single-modal network. The aim is to show that the triplet loss can be used for such a cross-modal setting in the field of common representation learning. Hence, we generate synthetic data where the image data contains information of the signal data. We generate signal data \mathbf{x} with $x_{i,k} = \sin(0.05 \cdot \frac{t_i}{k})$ for all $t_i \in \{1, \dots, 1,000\}$ where t_i is the timestep of the signal. The frequency of the signal is dependent on the class label k . We generate signal data for 10 classes (see Figure 9a). We add noise from a continuous uniform distribution $U(a, b)$ for $a = 0$ and $b = 0.3$ (see Figure 9b), and add time and magnitude warping (see Figure 9c). We generate a signal-image pair such that the image is based on the signal data. We make use of the Gramian angular field (GAF) that transforms time-series into images. The time-series is defined as $\mathbf{x} = (x_1, \dots, x_n)$ for $n = 1,000$. The GAF creates a matrix of temporal correlations for each (x_i, x_j) by rescaling the time-series in the range $[p, q]$ with $-1 \leq p < q \leq 1$ by

$$\hat{x}_i = p + (q - p) \cdot \frac{x_i - \min(\mathbf{x})}{\max(\mathbf{x}) - \min(\mathbf{x})}, \forall i \in \{1, \dots, n\}, \quad (4)$$

and computes the cosine of the sum of the angles for the Gramian angular summation field (GASF) Wang & Oates (2015) by

$$\text{GASF}_{i,j} = \cos(\phi_i + \phi_j), \forall i, j \in 1, \dots, n, \quad (5)$$

with $\phi_i = \arccos(\hat{x}_i)$, $\forall i \in \{1, \dots, n\}$, being the polar coordinates. We generate image datasets based on signal data with different noise parameters ($b \in \{0.0, \dots, 1.95\}$) to show the influence of the image data on the classification accuracy. Figure 10 exemplarily shows the GASF plots for the noise parameters $b = [0, 0.5, 1.0, 1.5, 1.95]$. We present the GASF for the classes 0, 5 and 9 to show the dependency of the frequency of the signal data on the GASF.

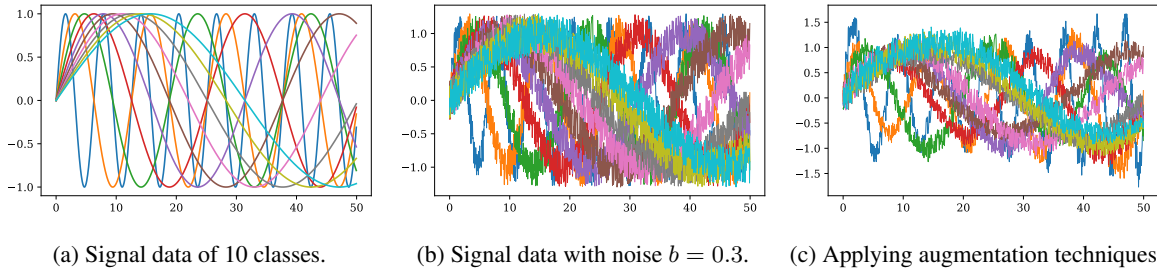


Figure 9: Plot of the 1D signal data for 10 classes.

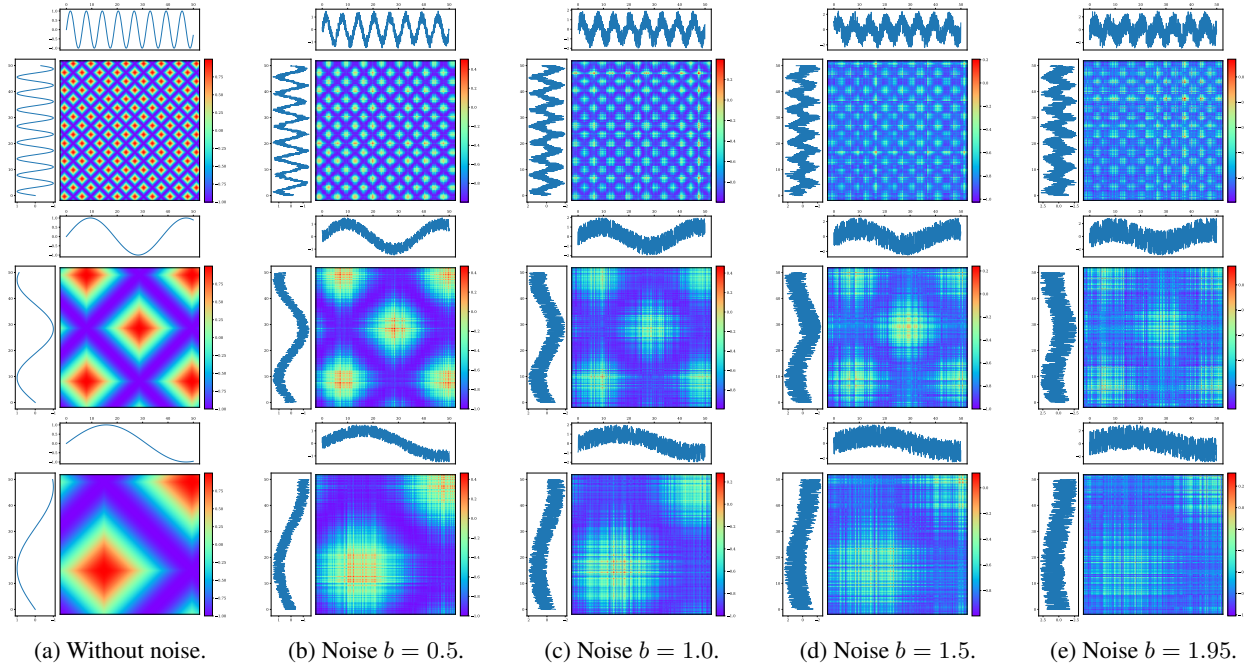


Figure 10: Plot of the Gramian angular summation field (GASF) based on 1D signal data with added noise for the classes 0 (top row), 5 (middle row) and 9 (bottom row).

Models. We use the following models for classification. Our encoder for time-series classification consists of a 1D convolutional layer (filter size 50, kernel 4), a max pooling layer (pool size 4), batch normalization, and a dropout layer (20%). The image encoder consists of a layer normalization and 2D convolutional layer (filter size 200), and batch normalization with ELU activation. It follows a 1D convolutional layer (filter size 200, kernel 4), max pooling (pool size 2), batch normalization, and 20% dropout. For both models, it follows a common representation, i.e., an LSTM with 10 units, a Dense layer with 20 units, a batch normalization layer, and a Dense layer of 10 units (for 10 sinusoidal classes). These layers are shared between both models.

A.3 Overview of Offline HWR Methods

In the following, we give a detailed overview of offline HWR methods to select a suitable lexicon and language model free method. There is no recent paper summarizing the work for offline HWR. For an overview of offline and online HWR datasets, see Plamondon & Srihari (2000); Hussain et al. (2015). Table 3 presents related work. Methods for offline HWR range from hidden markov models (HMMs) to deep learning techniques that became predominant such as convolutional neural networks (CNNs), temporal convolutional networks (TCNs) and recurrent neural networks (RNNs). RNN techniques are well explored including long short-term memories (LSTMs), bidirectional LSTMs (BiLSTMs), and multidimensional RNNs (MDRNN, MDLSTM). Recent methods are generative adversarial networks (GANs) and Transformers. We note the use of a language model (LM) and its size k , and the data level the method works with, i.e., paragraph or full text level (P), line level (L) and word level (W). We present evaluation results for the IAM-OffDB Liwicki & Bunke (2005) and RIMES Grosicki & El-Abed (2011) datasets including the word error rate (WER) and character error rate (CER).

HMMs. Methods based on HMMs from last decades are Bertolami & Bunke (2018); Dreuw et al. (2011); Li et al. (2014); Pastor-Pellicer et al. (2015). Recently, España-Boquera et al. (2011) proposed HMM+ANN, a HMM modeled with Markov chains in combination with a multilayer perceptron (MLP) to estimate the emission probabilities. Koziełski et al. (2013) presented Tandem GHMM that uses moment-based image normalization, writer adaptation and discriminative feature extraction with an 3-gram open-vocabulary of size 50k with an LSTM for recognition. Doetsch et al. (2014) proposed an LSTM unit that controls the shape of the squashing function in gating units decoded in a hybrid HMM. This approach yields the best results based on HMMs.

Table 3: Evaluation results (WER and CER in %) of different methods on the IAM-OffDB Liwicki & Bunke (2005) and RIMES Grosicki & El-Abed (2011) datasets. We state information about the method and the size of the language model (LM). LN = layer normalization. P = paragraph or full text level. L = line level. W = word level. The table is sorted by year.

	Method	Information	LM size k	Level P L W	IAM-OffDB WER CER	RIMES WER CER
HMM	HMM+ANN España-Boquera et al. (2011)	Markov chain with MLP	w/ (5)		15.50 6.90	- -
	Tandem GHMM Kozielski et al. (2013)	GHMM and LSTM, writer adaptation	w/ (50)	×	13.30 5.10	13.70 4.60
	LSTM-HMM Doetsch et al. (2014)	Combination of LSTM with HMM	w/ (50)	×	12.20 4.70	12.90 4.30
	2DLSTM Graves & Schmidhuber (2008)	Combined MDLSTM with CTC	w/o		27.50 8.30	17.70 4.00
	MDLSTM-RNN Bluche (2016)	150 dpi	w/o	×	29.50 10.10	13.60 3.20
		150 dpi	w/ (50)	×	16.60 6.50	- -
		300 dpi	w/o	×	24.60 7.90	12.60 2.90
		300 dpi	w/ (50)	×	16.40 5.50	- -
		GPU-based, diagonal MDLSTM			9.30 3.50	9.60 2.80
		Multi-task approach	w/o		34.55 11.15	30.54 8.29
Multi-dim. LSTM	MDLSTM Castro et al. (2018)	MDLSTM, attention	w/o	×	- 16.20	- -
	BiLSTM Graves et al. (2009)	Line segmentation 150 dpi	w/o	×	- 11.10	- -
	HMM+RNN Menasri et al. (2012)	Line segmentation 150 dpi	w/o	×	- 7.50	- -
	Dropout Pham et al. (2014)		w/ (20)		10.50 3.60	- -
	Voigtlaender et al. (2015)				18.20 25.90	- -
	Bluche (2015)	Sliding win. Gaussian HMM, RNN	w/o	×		4.75 -
		LSTMs with dropout	w/o		35.10 10.80	28.50 6.80
		Maximum mutual information			12.70 4.80	12.10 4.40
					10.90 4.40	11.20 3.50
					13.60 5.10	12.30 3.30
RNN	GCRNN Bluche & Messina (2017)	CNN+BiLSTM	w/ (50)		10.50 3.20	7.90 1.90
	CNN-1DLSTM-CTC Puigcerver (2017)	CNN+BiLSTM+CTC (128 x W)	w/o	×	18.40 5.80	9.60 2.30
	End2End Krishnan et al. (2018)	NN+BiLSTM+CTC	w/ (50)	×	12.20 4.40	9.00 2.50
	SFR Wigington et al. (2018)	Without line level	w/		16.19 6.34	- -
	CNN-RNN Dutta et al. (2018)	Line level	w/	×	32.89 9.78	- -
		Text detection and segmentation	w/o	×	23.20 6.40	9.30 2.10
		Unconstrained	w/o		12.61 4.88	7.04 2.32
		Full-Lexicon	w/		4.80 2.52	1.86 0.65
		Text-Lexicon	w/		4.07 2.17	
		Unconstrained	w/o	×	17.82 5.70	9.60 2.30
CNN	Chowdhury & Vig (2018)	Seq2seq, w/o LN	w/o		25.50 17.40	19.10 12.00
		w/ LN	w/o		22.90 13.10	15.80 9.70
		w/ LN + Focal Loss	w/o		21.10 11.40	13.50 7.30
		w/ LN + Focal Loss + Beam Search	w/o		16.70 8.10	9.60 3.50
	Sueiras et al. (2018)	LSTM encoder-decoder, attention			15.90 4.80	- -
	Chung & Delteil (2019)	ResNet+LSTM, segmentation	w/	×	- 8.50	- -
	Ingle et al. (2019)	BiLSTM		×	30.70 12.80	- -
	Michael et al. (2019)	GRCL		×	35.20 14.10	- -
	FPN Carbonell et al. (2019)	Seq2seq CNN+BiLSTM (64 x W)		×	- 5.24	- -
	AFDM Bhunia et al. (2019)	Feature Pyramid Network, 150 dpi		×	- 15.60	- -
GAN	Poznanski & Wolf (2016)	AFD module	w/		8.87 5.94	6.31 3.17
	GTR Yousef et al. (2018)	CNN + connected branches, CCA	w/		6.45 3.44	3.90 1.90
	OrigamiNet Yousef & Bishop (2020)	CNN+CTC (32 x W)	w/o	×	- 4.90	- -
		VGG (500x500)	x	×	- 51.37	- -
		VGG (500x500), w/o LN	w/o	×	- 34.55	- -
		ResNet26 (500x500), w/o LN	w/o	×	- 10.03	- -
		ResNet26 (500x500), w/ LN	w/o	×	- 7.24	- -
		ResNet26 (500x500), w/o LN	w/o	×	- 8.93	- -
		ResNet26 (500x500), w/ LN	w/o	×	- 6.37	- -
		ResNet26 (500x500), w/o LN	w/o	×	- 76.90	- -
Trans-former	DAN Wang et al. (2020)	ResNet26 (500x500), w/ LN	w/o	×	- 6.13	- -
	ScrabbleGAN Fogel et al. (2020)	GTR-8 (500x500), w/o LN	w/o	×	- 72.40	- -
		GTR-8 (500x500), w/ LN	w/o	×	- 5.64	- -
		GTR-8 (750x750), w/ LN	w/o	×	- 5.50	- -
		GTR-12 (750x750), w/ LN	w/o	×	- 4.70	- -
		Decoupled attention module	w/o	×	19.60 6.40	8.90 2.70
		Original data	w/o		25.10 -	12.29 -
		Augm.	w/o		24.73 -	12.24 -
		Augm + 100k synth.	w/o		23.98 -	11.68 -
		Augm + 100k synth. + Refine	w/o		23.61 -	11.32 -
Other	Kang et al. (2020)	Self-attention for text/images	w/o	×	15.45 4.67	- -
	FPHR Singh & Karayev (2021)	CNN encoder, Transformer decoder	w/o	×	- 6.70	- -
		With augmentation	w/o	×	- 6.30	- -
	FST Messina & Kermorvant (2014)	Finite state transducer (lexicon)	n-gram		19.10 -	13.30 -

RNNs: MDLSTMs. The 2DLSTM approach by Graves & Schmidhuber (2008) combines multidimensional LSTMs (MDLSTMs) with the CTC loss. The MDLSTM-RNN approach Bluche (2016) works at paragraph level by replacing the collapse layer by a recurrent version. A neural network performs implicit line segmentation by computing attention weights on the image representation. Voigtlaender et al. (2016) proposed an efficient GPU-based implementation of MDLSTMs by processing the input in a diagonal-wise fashion. SepMDLSTM Chen et al. (2017) is a multi-task learning method for script identification and HWR based on two classification modules by minimizing the CTC and negative log likelihood losses. While the MDLSTM by Bluche et al. (2017) contains covert and overt attention without prior segmentation, the Castro et al. (2018) integrated MDLSTMs within a hybrid HMM. However, these architectures come with quite an expensive computational cost. Furthermore, they extract features visually similar to those of convolutional layers Puigcerver (2017). End2End Krishnan et al. (2018) jointly learns text and image embeddings based on LSTMs.

RNNs: LSTMs and BiLSTMs. RNNs for HWR marked an important milestone reaching impressive recognition accuracies. Sequential architectures are perfect to fit text lines due to the probability distributions over sequences of characters and due to the inherent temporal aspect of text Kang et al. (2020). Graves et al. (2009) introduced the BiLSTM layer in combination with the CTC loss. Pham et al. (2014) showed that the performance of LSTMs can be greatly improved using dropout. Voigtlaender et al. (2015) investigated sequence-discriminative training of LSTMs using the maximum mutual information (MMI) criterion. While Bluche (2015) utilized a RNN with a HMM and a language model, Menasri et al. (2012) combined a RNN with a sliding window Gaussian HMM. GCRNN Bluche & Messina (2017) combines a convolutional encoder (aiming generic and multilingual features) and a BiLSTM decoder predicting character sequences. Also, Puigcerver (2017) proposed a CNN+BiLSTM architecture (CNN-1DLSTM-CTC) that uses the CTC loss. The start, follow, read (SFR) Wigington et al. (2018) model jointly learns text detection and segmentation. Dutta et al. (2018) used synthetic data for pre-training and image normalization for slant correction. The methods by Chowdhury & Vig (2018); Sueiras et al. (2018); Ingle et al. (2019); Michael et al. (2019) make also use of BiLSTMs. While Carbonell et al. (2019) uses a feature pyramid network (FPN), the adversarial feature deformation module (AFDM) Bhunia et al. (2019) learns ways to elastically warp extracted features in a scalable manner. Further methods that combine CNNs with RNNs are Liang et al. (2017); Sudholt & Fink (2018); Xiao & Cho (2016), while BiLSTMs are utilized in Carbune et al. (2020); Tian et al. (2019).

TCNs. TCNs uses dilated causal convolutions and have been applied to air-writing recognition by Bastas et al. (2020). As RNNs are slow to train, Sharma et al. (2020) presented a faster system which is based on text line images and TCNs with the CTC loss. This method achieves 9.6% CER on the IAM-OffDB dataset. Sharma & Jayagopi (2021) combined 2D convolutions with 1D dilated non-causal convolutions that offers a high parallelism with a smaller number of parameters. They analyzed re-scaling factors and data augmentation, and achieved comparable results for the IAM-OffDB and RIMES datasets.

CNNs. Poznanski & Wolf (2016) utilized a CNN with multiple fully connected branches to estimate its n-gram frequency profile (set of n-grams contained in the word). With canonical correlation analysis (CCA), the estimated profile can be matched to the true profiles of all words in a large dictionary. As most attention methods suffer from an alignment problem, Wang et al. (2020) proposed a decoupled attention network (DAN) that has a convolutional alignment module that decouples the alignment operation from using historical decoding results based on visual features. The gated text recognizer (GTR) Yousef et al. (2018) aims to automate the feature extraction from raw input signal with minimum required domain knowledge. The fully convolutional network without recurrent connections is trained with the CTC loss. Thus, the GTR module can handle arbitrary input sizes and can recognize strings with arbitrary length. This module has been used for OrigamiNet Yousef & Bishop (2020) that is a segmentation-free multi-line or full page recognition system. OrigamiNet yields state-of-the-art results on the IAM-OffDB dataset, and shows an improved performance of GTR over VGG and ResNet26. Hence, we use the GTR module as our visual feature encoder for offline HWR (see Section A.4).

GANs. Handwriting text generation (HTG) is a relatively new field. The first approach by Graves (2014) was a method to synthesize online data based on RNNs. The technique HWGAN by Ji & Chen (2020) extends this method by adding a discriminator \mathcal{D} . DeepWriting Aksan et al. (2016) is a GAN that is capable of disentangling style from content and thus making digital ink editable. Haines et al. (2016) proposed a method to generate handwriting based on a specific author with learned parameters for spacing, pressure and line thickness. Alonso et al. (2019) used a

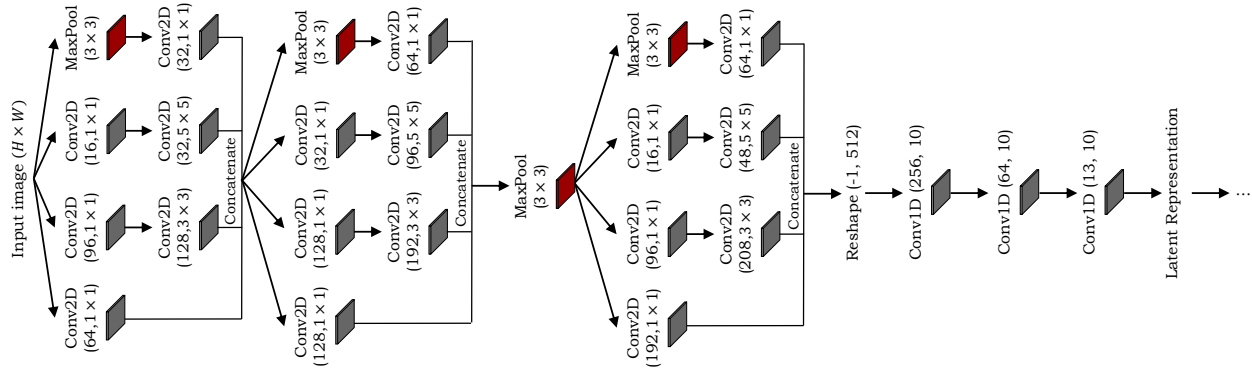


Figure 11: Offline HWR method based on Inception modules Szegedy et al. (2015).

BiLSTM to get an embedding of the word to be rendered, and added an auxiliary network as recognizer \mathcal{R} . The model is trained with a combination of an adversarial loss and the CTC loss. ScrabbleGAN by Fogel et al. (2020) is a semi-supervised approach that can generate arbitrarily many images of words with arbitrary length from a generator \mathcal{G} to augment handwriting data and uses a discriminator \mathcal{D} and recognizer \mathcal{R} . The paper proposes results for original data, with random affine augmentation, using synthetic images and refinement.

Transformers. RNNs prevent parallelization due to their sequential pipelines. Kang et al. (2020) introduced a non-recurrent model by the use of Transformer models by using multi-head self-attention layers at the textual and visual stages. Their method is unconstrained to any pre-defined vocabulary. For the feature encoder, they used modified ResNet50 models. The full page HTR (FPHR) method by Singh & Karayev (2021) uses a CNN as encoder and a Transformer as decoder with positional encoding.

A.4 Details on Architectures for Offline HWR

In this section, we give details about the integration of Inception Szegedy et al. (2015), ResNet He et al. (2016) and GTR Yousef et al. (2018) modules into the offline HWR system. All three architectures are based on publicly available implementations, but we changed or adapted the first layer for the image input and the last layer for a proper input for our latent representation module.

Inception. Figure 11 gives an overview of the integration of the Inception module. The Inception module is part of the well known GoogLeNet architecture. The main idea is to consider how an optimal local sparse structure can be approximated by readily available dense components. As the merging of pooling layer outputs with convolutional layer outputs would lead to an inevitable increase in the number of output and would lead to computational blow up, we apply the Inception module with dimensionality reduction to our offline HWR approach Szegedy et al. (2015). The input image is of size $H \times W$. What follows is the Inception (3a), Inception (3b), a max pooling layer (3×3) and Inception (4a). We add three 1D convolutional layers to get an output dimensionality of 400×200 as input for the latent representation.

ResNet34. Figure 12 gives an overview of the integration of the ResNet34 architecture. Instead of learning unreferenced functions, He et al. (2016) reformulated the layers as learning residual functions with reference to the layer inputs. This residual network is easier to optimize and can gain accuracy from considerably increased depth. The ResNet block let the layers fit a residual mapping denoted as $\mathcal{H}(\mathbf{x})$ with identity \mathbf{x} , and fits the mapping $\mathcal{F}(\mathbf{x}) := \mathcal{H}(\mathbf{x}) - \mathbf{x}$. The original mapping is recast into $\mathcal{F}(\mathbf{x}) + \mathbf{x}$. We reshape the output of ResNet34, add a 1D convolutional layer, and reshape the output for the latent representation.

GTR. Figure 13 gives an overview of the integration of the gated text recognizer (GTR) Yousef et al. (2018) module that is a fully convolutional network that uses batch normalization (BN) and layer normalization (LN) to regularize the training process and increase convergence speed. The module uses batch renormalization Ioffe (2017) on all BN layers. Depthwise separable convolutions reduce the number of parameters at the same/better classification performance.

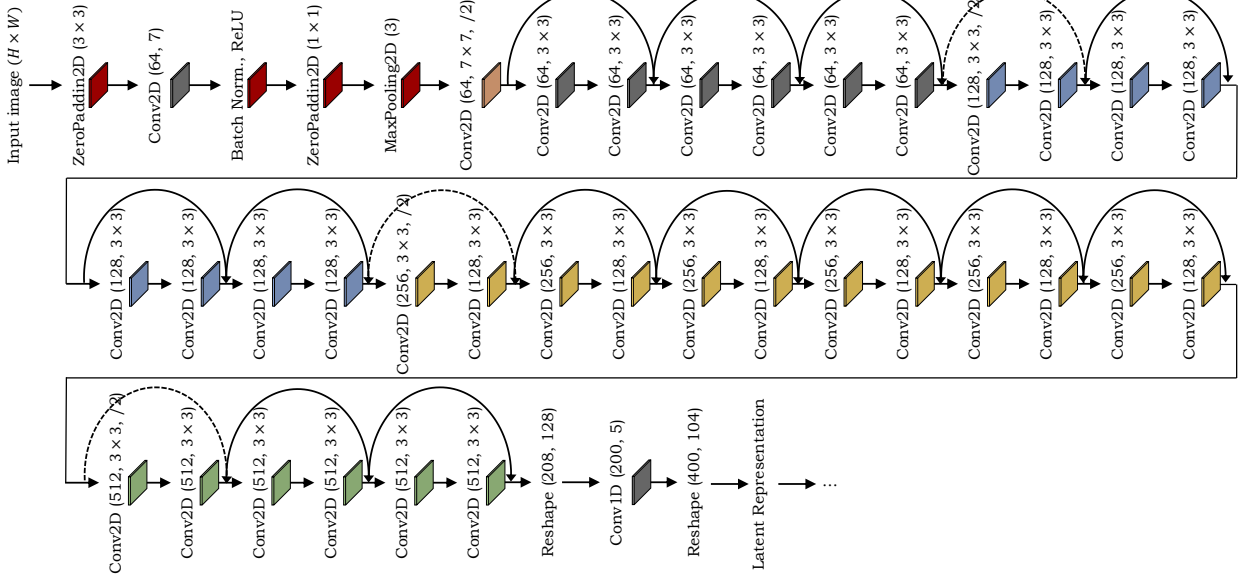


Figure 12: Offline HWR method based on the ResNet34 architecture He et al. (2016).

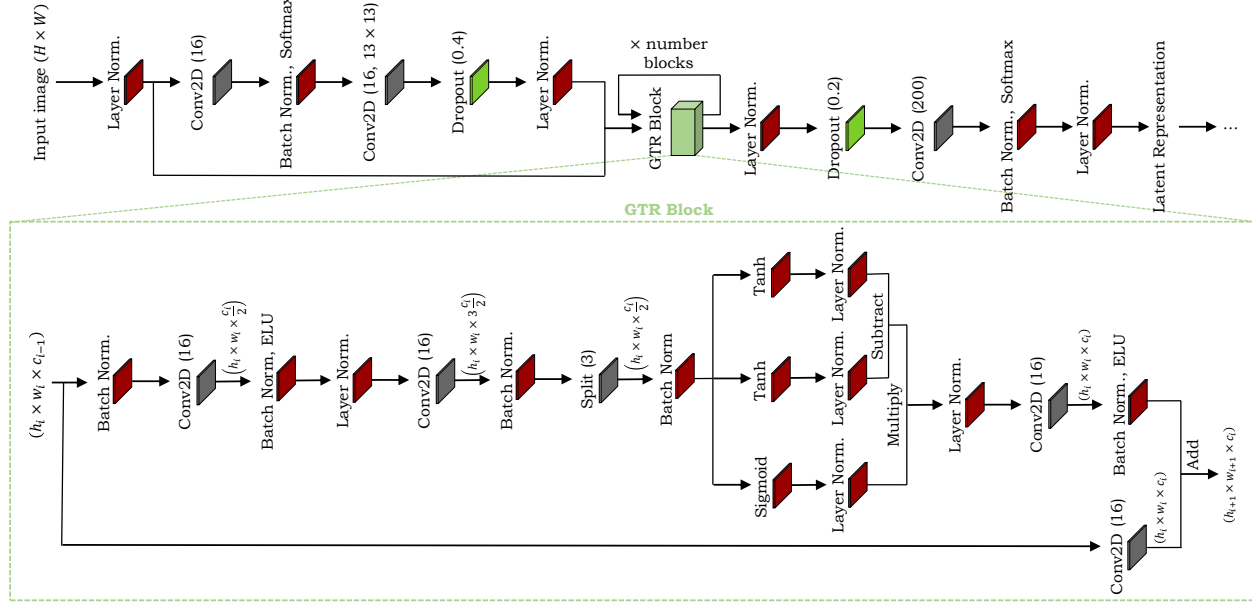


Figure 13: Offline HWR method based on the GTR architecture Yousef et al. (2018).

GTR uses spatial dropout instead of regular unstructured dropout for better regularization. After the input image of size $H \times W$ that is normalized follows a convolutional layer with Softmax normalization, a 13×13 filter, and dropout (40%). It follows a stack of 2, 4, 6 or 8 gate blocks that models the input sequence. Similar as Yousef et al. (2018), we add a dropout of 20% after the last GTR block. Lastly, we add a 2D convolutional layer of 200, a BN layer and a LN layer that is the input for our latent representation.

A.5 Detailed HWR Evaluation

Offline HWR Results. Table 4 shows offline HWR results on our generated OffHW-German dataset and on the IAM-OffDB Liwicki & Bunke (2005) dataset. ScrabbleGAN Fogel et al. (2020) yields an WER of 23.61% on the

Table 4: Evaluation results (WER and CER in %) for the generated dataset with ScrabbleGAN Fogel et al. (2020) OffHW-German and the IAM-OffDB Liwicki & Bunke (2005) dataset. We propose writer-dependent (WD) and writer-independent (WI) results.

Method	OffHW-German		IAM-OffDB	
	WER	CER	WER	CER
ScrabbleGAN Fogel et al. (2020)	-	-	23.61	-
OrigamiNet (12×GTR) Yousef & Bishop (2020)	-	-	-	4.70
OrigamiNet (ours, 4×GTR)	1.50	0.11	90.40	15.67
Inception	12.54	1.17	-	-
ResNet	13.05	1.24	-	-
GTR (2 blocks), 1 conv. layer	4.34	0.39	-	-
GTR (2 blocks), 2 conv. layer	5.02	0.44	-	-
GTR (4 blocks), 1 conv. layer	3.35	0.34	89.37	15.60
GTR (4 blocks), 2 conv. layer	2.52	0.24	-	-
GTR (6 blocks)	2.85	0.26	-	-
GTR (8 blocks)	4.22	0.38	-	-

Table 5: Evaluation results (WER and CER in %) for the generated OffHW-words500 and OffHW-wordsRandom datasets for one and two convolutional layers (c). We propose writer-dependent (WD) and writer-independent (WI) results.

Method (4×GTR)	OffHW-words500				OffHW-wordsRandom			
	WD		WI		WD		WI	
	WER	CER	WER	CER	WER	CER	WER	CER
$c = 1$	2.94	0.76	0.95	0.23	1.98	0.35	2.05	0.37
$c = 2$	2.51	0.69	0.85	0.22	1.82	0.34	1.95	0.38

IAM dataset, while OrigamiNet Yousef & Bishop (2020) achieves an CER of 4.70% with 12 GTR modules. As the training takes more than one day for one epoch on the large OffHW-German dataset, we train OrigamiNet with four GTR modules, and achieve 0.11% CER on the generated dataset and 15.67% on the IAM dataset, which is higher than the model with 12 GTR modules. While the paper did not propose WER results, OrigamiNet yields only an WER of 90.40%. With our own implementation of four GTR modules and one convolutional layer for the common representation, our model achieves similar results. While GTR modules yield slightly lower CERs on the OffHW-German dataset than our architectures with Inception and ResNet modules, the WERs are significantly higher. Fine-tuning the architecture with four GTR modules and one ($c = 1$) or two ($c = 2$) convolutional layers on the OffHW-words500 and OffHW-wordsRandom datasets, yields better results for $c = 2$ than for $c = 1$ (see Table 5). While results for OffHW-wordsRandom are similar for writer-dependent (WD) and writer-independent (WI), WI results of the OffHW-words500 dataset are lower than WD results, as words with the same label appear in the training and test dataset. We use the weights of the fine-tuning as initial weights of the image model for the common representation learning.

Online HWR Results. Table 2 gives an overview of CRL results based on two convolutional layers ($c = 2$) for the common representation. Our CNN+BiLSTM contains three additional convolutional layers and outperforms the smaller CNN+BiLSTM by Ott et al. (2022) on the WD classification tasks. Without triplet loss, \mathcal{L}_{PC} yields the best results on the OnHW-wordsRandom dataset. The triplet loss partly marginally decreases results and partly improves results on the OnHW-words500 dataset. In conclusion, two convolutional layers for the common representation decreases results, while here the triplet loss does not have a positive impact.

Table 6: Evaluation results (WER and CER in %, averaged over five splits) of the baseline MTS-only technique and our cross-modal techniques for the inertial-based OnHW datasets Ott et al. (2022) with and without mutated vowels (MV) for two convolutional layers $c = 2$. We propose writer-(in)dependent (WD/WI) results.

Method	OnHW-words500				OnHW-wordsRandom			
	WD		WI		WD		WI	
	WER	CER	WER	CER	WER	CER	WER	CER
Small CNN+BiLSTM, \mathcal{L}_{CTC} , w/ MV	51.95	17.16	60.91	27.80	41.27	7.87	84.52	35.22
CNN+BiLSTM (ours), \mathcal{L}_{CTC} , w/ MV	42.81	13.04	60.47	28.30	37.13	6.75	83.28	35.90
CNN+BiLSTM (ours), \mathcal{L}_{CTC} , w/o MV	42.77	13.44	59.82	28.54	41.52	7.81	83.54	36.51
\mathcal{L}_{MSE}	39.79	12.14	60.35	28.48	39.98	7.79	83.50	36.92
\mathcal{L}_{CS}	43.40	13.70	59.31	27.99	40.31	7.68	83.68	36.30
\mathcal{L}_{PC}	38.90	11.60	60.77	28.45	39.93	7.60	83.19	35.83
\mathcal{L}_{KL}	37.25	11.29	65.10	31.26	41.81	8.22	84.40	38.93
$\mathcal{L}_{\text{trpl,2}}(\mathcal{L}_{\text{MSE}})$	41.16	12.71	58.65	28.19	41.16	8.03	85.38	39.49
$\mathcal{L}_{\text{trpl,2}}(\mathcal{L}_{\text{CS}})$	42.74	13.43	58.13	27.62	41.49	8.18	85.24	38.75
$\mathcal{L}_{\text{trpl,2}}(\mathcal{L}_{\text{PC}})$	39.94	12.19	62.76	30.68	41.58	8.18	85.18	38.53
$\mathcal{L}_{\text{trpl,2}}(\mathcal{L}_{\text{KL}})$	38.34	11.77	67.08	33.84	41.87	8.33	86.34	40.37

Table 7: Evaluation results (WER and CER in %, averaged over five splits) of the baseline MTS-only technique and our cross-modal techniques for the inertial-based OnHW datasets Ott et al. (2022) with and without mutated vowels (MV) for two convolutional layers $c = 1$. We propose writer-(in)dependent (WD/WI) results.

Method	OnHW-words500-L				OnHW-wordsRandom-L			
	WD		WI		WD		WI	
	WER	CER	WER	CER	WER	CER	WER	CER
InceptionTime, \mathcal{L}_{CTC} , w/ MV	49.70	14.02	100.00	96.06	48.10	8.63	100.00	95.93
CNN+BiLSTM, \mathcal{L}_{CTC} , w/ MV	14.20	3.30	94.40	71.41	30.20	4.86	100.00	83.51
CNN+BiLSTM, \mathcal{L}_{CTC} , w/o MV	12.94	3.33	89.07	62.07	30.89	5.26	100.00	81.15
\mathcal{L}_{MSE}	11.62	2.77	90.65	67.90	30.53	4.93	100.00	81.99
\mathcal{L}_{CS}	14.92	3.53	94.14	65.10	29.06	4.87	100.00	83.94
\mathcal{L}_{PC}	12.29	3.04	91.33	60.89	27.32	4.47	100.00	85.09
\mathcal{L}_{KL}	11.37	2.57	93.02	66.64	29.61	4.91	100.00	81.28
$\mathcal{L}_{\text{trpl,2}}(\mathcal{L}_{\text{MSE}})$	11.97	2.83	84.34	57.84	27.19	4.79	99.87	82.60
$\mathcal{L}_{\text{trpl,2}}(\mathcal{L}_{\text{CS}})$	11.65	2.63	94.70	67.69	28.39	4.62	100.00	83.44
$\mathcal{L}_{\text{trpl,2}}(\mathcal{L}_{\text{PC}})$	13.02	2.94	89.86	60.26	30.22	4.81	100.00	84.29
$\mathcal{L}_{\text{trpl,2}}(\mathcal{L}_{\text{KL}})$	13.55	3.22	97.86	76.54	28.14	4.71	100.00	80.81

Transfer Learning on Left-Handed Writers. To adapt the model to left-handed writers that are typically under-represented in the real-world, we make use of the left-handed datasets OnHW-words500-L and OnHW-wordsRandom-L proposed by Ott et al. (2022). These datasets contain recordings of two writers with 1,000 samples, respectively 996. As baseline we pre-train the MTS-only model on the right-handed datasets and post-train the left-handed datasets for 500 epochs (see the first two rows of Table 7). As these datasets are rather small, the models can overfit on these specific writers and achieve a very low CER of 3.33% on the OnHW-words500-L dataset and 5.26% CER on the OnHW-wordsRandom-L dataset without mutated vowels (MV) for the writer-dependent (WD) tasks, but the models can not generalize on the writer-independent (WI) tasks: 62.07% CER on the OnHW-words500-L dataset and 81.15% CER on the OnHW-wordsRandom-L dataset. Hence, we focus on the WD tasks. For comparison, we use the state-of-the-art time-series classification technique InceptionTime Fawaz et al. (2019) with $depth = 11$ and $nf = 96$ (without pre-training). Our CNN+BiLSTM clearly outperforms InceptionTime. We use the weights of the pre-training with the offline handwriting datasets and again post-train on the left-handed datasets with $c = 1$. Using the weights of the cross-modal learning without the triplet loss, can decrease the error rates up to 2.57% CER with \mathcal{L}_{KL} , respectively 4.47% CER with \mathcal{L}_{PC} . Using the triplet loss $\mathcal{L}_{\text{trpl,2}}(\mathcal{L}_{\text{CS}})$, we can further decrease the CER to 2.63% for the OnHW-words500-L dataset. In conclusion, due to the use of the weights of the cross-modal setup, the model can adapt faster to new writers and generalize better to unseen words due to the triplet loss.

References

- Emre Aksan, Fabrizio Pece, and Otmar Hilliges. DeepWriting: Making Digital Ink Editable via Deep Generative Modeling. In *arXiv preprint arXiv:11801.08379*, January 2016.
- Eloi Alonso, Bastien Moysset, and Ronaldo Messina. Adversarial Generation of Handwritten Text Images Conditioned on Sequences. In *Intl. Conf. on Document Analysis and Recognition (ICDAR)*, Sydney, Australia, September 2019.
- Grigoris Bastas, Kosmas Kritsis, and Vassilis Katsouros. Air-Writing Recognition using Deep Convolutional and Recurrent Neural Network Architectures. In *Intl. Conf. on Frontiers in Handwriting Recognition (ICFHR)*, pp. 7–12, September 2020.
- Roman Bertolami and Horst Bunke. Hidden Markov Model-based Ensemble Methods for Offline Handwritten Text Line Recognition. In *Pattern Recognition*, volume 41(11), pp. 3452–3460, November 2018.
- Ayan Kumar Bhunia, Abhirup Das, Ankan Kumar Bhunia, Perla Sai Raj Kishore, and Partha Pratim Roy. Handwriting Recognition in Low-Resource Scripts Using Adversarial Learning. In *Intl. Conf. on Computer Vision and Pattern Recognition (CVPR)*, Long Beach, CA, June 2019.
- Théodore Bluche. Deep Neural Networks for Large Vocabulary Handwritten Text Recognition. In *Thèse de Doctorat*, Université Paris-Sud, 2015.
- Théodore Bluche. Joint Line Segmentation and Transcription for End-to-End Handwritten Paragraph Recognition. In *Advances in Neural Information Processing Systems (NIPS)*, pp. 838–846, December 2016.
- Théodore Bluche and Ronaldo Messina. Gated Convolutional Recurrent Neural Networks for Multilingual Handwriting Recognition. In *Intl. Conf. on Document Analysis and Recognition (ICDAR)*, pp. 646–651, November 2017.
- Théodore Bluche, Jérôme Louradour, and Ronaldo Messina. Scan, Attend and Read: End-to-End Handwritten Paragraph Recognition with MDLSTM Attention. In *Intl. Conf. on Document Analysis and Recognition (ICDAR)*, Kyoto, Japan, November 2017.
- Manuel Carbonell, Joan Mas, Mauricio Villegas, Alicia Fornés, and Josep Lladós. End-to-End Handwritten Text Detection and Transcription in Full Pages. In *Intl. Conf. on Document Analysis and Recognition Workshops (ICDARW)*, Sydney, Australia, September 2019.
- Victor Carbune, Pedro Gonnet, Thomas Deselaers, Henry A. Rowley, Alexander Daryin, Marcos Calvo, Li-Lun Wang, Daniel Keysers, Sandro Feuz, and Philippe Gervais. Fast Multi-language LSTM-based Online Handwriting Recognition. In *Intl. Journal on Document Analysis and Recognition (IJDAR)*, volume 23, pp. 89–102, February 2020.
- Dayvid Castro, Byron L. D. Bezerra, and Mêuser Valença. Boosting the Deep Multidimensional Long-Short-Term Memory Network for Handwritten Recognition Systems. In *Intl. Conf. on Frontiers in Handwriting Recognition (ICFHR)*, Niagara Falls, NY, August 2018.
- Zhuo Chen, Yichao Wu, Fei Yin, and Cheng-Lin Liu. Simultaneous Script Identification and Handwriting Recognition via Multi-Task Learning of Recurrent Neural Networks. In *Intl. Conf. on Document Analysis and Recognition (ICDAR)*, pp. 525–530, November 2017.
- Arindam Chowdhury and Lovekesh Vig. An Efficient End-to-End Neural Model for Handwritten Text Recognition. In *British Machine Vision Conference (BMVC)*, 2018.
- Jonathan Chung and Thomas Delteil. A Computationally Efficient Pipeline Approach to Full Page Offline Handwritten Text Recognition. In *Intl. Conf. on Document Analysis and Recognition Workshops (ICDARW)*, Sydney, Australia, September 2019.
- Patrick Doetsch, Michal Kozielski, and Hermann Ney. Fast and Robust Training of Recurrent Neural Networks for Offline Handwriting Recognition. In *Intl. Conf. on Frontiers in Handwriting Recognition (ICFHR)*, Hersonissos, Greece, September 2014.

Philippe Dreuw, Patrick Doetsch, Christian Plahl, and Hermann Ney. Hierarchical Hybrid MLP/HMM or Rather MLP Features for a Discriminatively Trained Gaussian HMM: A Comparison for Offline Handwriting Recognition. In *Intl. Conf. on Image Processing (ICIP)*, Brussels, Belgium, September 2011.

Kartik Dutta, Praveen Krishnan, Minesh Mathew, and C. V. Jawahar. Improving CNN-RNN Hybrid Networks for Handwriting Recognition. In *Intl. Conf. on Frontiers in Handwriting Recognition (Intl. Conf. on Frontiers in Handwriting Recognition (ICFHR))*, pp. 80–85, 2018.

S. España-Boquera, M.J. Castro-Bleda, J. Gorbe-Moya, and F. Zamora-Martinez. Improving Offline Handwritten Text Recognition with Hybrid HMM/ANN Models. In *Trans. on Pattern Analysis and Machine Intelligence (TPAMI)*, volume 33(4), pp. 767–779, April 2011.

Hassan Ismail Fawaz, Benjamin Lucas, Germain Forestier, Charlotte Pelletier, Daniel F. Schmidt, Jonathan Weberf, Geoffrey I. Webb, Lhassane Idoumghar, Pierre-Alain Muller, and François Petitjean. InceptionTime: Finding AlexNet for Time Series Classification. In *arXiv preprint arXiv:1909.04939*, September 2019.

Sharon Fogel, Hadar Averbuch-Elor, Sarel Cohen, Shai Mazor, and Roee Litman. ScrabbleGAN: Semi-Supervised Varying Length Handwritten Text Generation. In *Intl. Conf. on Computer Vision and Pattern Recognition (CVPR)*, pp. 4324–4333, June 2020.

Alex Graves. Generating Sequences with Recurrent Neural Networks. In *arXiv preprint arXiv:1308.0850*, June 2014.

Alex Graves and Jürgen Schmidhuber. Offline Handwriting Recognition with Multidimensional Recurrent Neural Networks. In *Advances in Neural Information Processing Systems (NIPS)*, pp. 545–552, 2008.

Alex Graves, Marcus Liwicki, Santiago Fernández, Roman Bertolami, Horst Bunke, and Jürgen Schmidhuber. A Novel Connectionist System for Unconstrained Handwriting Recognition. In *Trans. on Pattern Analysis and Machine Intelligence (TPAMI)*, volume 31(5), pp. 855–868, May 2009.

Emmanuele Grosicki and Haikal El-Abed. ICDAR 2011 - French Handwriting Recognition Competition. In *Intl. Conf. on Document Analysis and Recognition (ICDAR)*, Beijing, China, 2011.

Tom S. F. Haines, Oisin Mac Aodha, and Gabriel J. Brostow. My Text in Your Handwriting. In *ACM Trans. on Graphics*, volume 35(3), pp. 1–18, May 2016.

Kaiming He, Xiangyu Zhang, Shaoqing Ren, and Jian Sun. Deep Residual Learning for Image Recognition. In *Intl. Conf. on Computer Vision and Pattern Recognition (CVPR)*, Las Vegas, NV, June 2016.

Raashid Hussain, Ahsen Raza, Imran Siddiqi, Khurram Khurshid, and Chawki Djeddi. A Comprehensive Survey of Handwritten Document Benchmarks: Structure, Usage and Evaluation. In *Journal on Image and Video Processing*, volume 46, 2015.

R. Reeve Ingle, Yasuhisa Fujii, Thomas Deselaers, Jonathan Baccash, and Ashok C. Popat. A Scalable Handwritten Text Recognition System. In *Intl. Conf. on Document Analysis and Recognition (ICDAR)*, Sydney, Australia, September 2019.

Sergey Ioffe. Batch Renormalization: Towards Reducing Minibatch Dependence in Batch-Normalized Models. In *Advances in Neural Information Processing Systems (NIPS)*, 2017.

Bo Ji and Tianyi Chen. Generative Adversarial Network for Handwritten Text. In *arXiv preprint arXiv:1907.11845*, February 2020.

Lei Kang, Pau Riba, Marcal Rusinol, Alicia Fornes, and Mauricio Villegas. Pay Attention to What You Read: Non-recurrent Handwritten Text-Line Recognition. In *arXiv preprint arXiv:2005.13044*, May 2020.

Michał Koziełski, Patrick Doetsch, and Hermann Ney. Improvements in RWTH’s System for Off-Line Handwriting Recognition. In *Intl. Conf. on Document Analysis and Recognition (ICDAR)*, Washington, DC, August 2013.

Praveen Krishnan, Kartik Dutta, and C. V. Jawahar. Word Spotting and Recognition using Deep Embedding. In *Intl. Workshop on Document Analysis Systems (DAS)*, pp. 1–6, 2018.

- Nan Li, Jinying Chen, Huagu Cao, Bing Zhang, and Prem Natarajan. Applications of Recurrent Neural Network Language Model in Offline Handwriting Recognition and Word Spotting. In *Intl. Conf. on Frontiers in Handwriting Recognition (ICFHR)*, Hersonissos, Greece, September 2014.
- Dongyun Liang, Weiran Xu, and Ying Zhao. Combining Word-Level and Character-Level Representations for Relation Classification of Informal Text (RepL4NLP). In *Workshop on Representation Learning for NLP*, pp. 43–47, Vancouver, Canada, August 2017.
- Shikun Liu, Edward Johns, and Andrew J. Davison. End-to-End Multi-Task Learning with Attention. In *Intl. Conf. on Computer Vision and Pattern Recognition (CVPR)*, pp. 1871–1880, Long Beach, CA, June 2019.
- Marcus Liwicki and Horst Bunke. IAM-OnDB - an On-Line English Sentence Database Acquired from Handwritten Text on a Whiteboard. In *Intl. Conf. on Document Analysis and Recognition (ICDAR)*, pp. 956–961, Seoul, Korea, August 2005.
- Farès Menasri, Jérôme Louradour, Anne-Laure Bianne-Bernard, and Christopher Kermorvant. The A2iA French Handwriting Recognition System at the RIMES-ICDAR2011 Competition. In *Proc. of the Intl. Society for Optical Engineering (SPIE)*, volume 8297, January 2012.
- Ronaldo Messina and Christopher Kermorvant. Over-Generative Finite State Transducer N-Gram for Out-of-Vocabulary Word Recognition. In *Intl. Workshop on Document Analysis Systems*, Tours, France, April 2014.
- Johannes Michael, Roger Labahn, Tobias Grüning, and Jochen Zöllner. Evaluating Sequence-to-Sequence Models for Handwritten Text Recognition. In *Intl. Conf. on Document Analysis and Recognition (ICDAR)*, September 2019.
- Felix Ott, David Rügamer, Lucas Heublein, Tim Hamann, Jens Barth, Bernd Bischl, and Christopher Mutschler. Benchmarking Online Sequence-to-Sequence and Character-based Handwriting Recognition from IMU-Enhanced Pens. In *arXiv preprint arXiv:2202.07036*, February 2022.
- Joan Pastor-Pellicer, Salvador Espana-Boquera, M. J. Castro-Bleda, and Francisco Zamora-Martínez. A Combined Convolutional Neural Network and Dynamic Programming Approach for Text Line Normalization. In *Intl. Conf. on Document Analysis and Recognition (ICDAR)*, Tunis, Tunisia, August 2015.
- Vu Pham, Théodore Bluche, Christopher Kermorvant, and Jérôme Louradour. Dropout Improves Recurrent Neural Networks for Handwriting Recognition. In *Intl. Conf. on Frontiers in Handwriting Recognition (ICFHR)*, pp. 285–290, 2014.
- Rejean Plamondon and Sargur N. Srihari. On-line and Off-line Handwriting Recognition: A Comprehensive Survey. In *Trans. on Pattern Analysis and Machine Intelligence (TPAMI)*, volume 22(1), pp. 63–84, January 2000.
- Arik Poznanski and Lior Wolf. CNN-N-Gram for Handwriting Word Recognition. In *Intl. Conf. on Computer Vision and Pattern Recognition (CVPR)*, pp. 2306–2314, Las Vegas, NV, June 2016.
- Joan Puigcerver. Are Multidimensional Recurrent Layers Really Necessary for Handwritten Text Recognition? In *Intl. Conf. on Document Analysis and Recognition (ICDAR)*, pp. 67–72, 2017.
- Annapurna Sharma and Dinesh Babu Jayagopi. Towards Efficient Unconstrained Handwriting Recognition using Dilated Temporal Convolutional Network. In *Expert Systems with Applications*, volume 164, February 2021.
- Annapurna Sharma, Rahul Ambati, and Dinesh Babu Jayagopi. Towards Faster Offline Handwriting Recognition using Temporal Convolutional Networks. In *National Conf. on Computer Vision, Pattern Recognition, Image Processing, and Graphics (NCVPRIPG)*, pp. 344–354, November 2020.
- Sumeet S. Singh and Sergey Karayev. Full Page Handwriting Recognition via Image to Sequence Extraction. In *arXiv preprint arXiv:2103.06450*, March 2021.
- Sebastian Sudholt and Gernot A. Fink. Attribute CNNs for Word Spotting in Handwritten Documents. In *Intl. Journal on Document Analysis and Recognition (IJDAR)*, volume 21, pp. 199–218, February 2018.

- Jorge Sueiras, Victoria Ruiz, Angel Sanchez, and Jose F. Velez. Offline Continuous Handwriting Recognition Using Sequence-to-Sequence Neural Networks. In *Neurocomputing*, volume 289(C), pp. 119–128, May 2018.
- Christian Szegedy, Wei Liu, Yangqing Jia, Pierre Sermanet, Scott Reed, Dragomir Anguelov, Dumitru Erhan, Vincent Vanhoucke, and Andrew Rabinovich. Going Deeper with Convolutions. In *Intl. Conf. on Computer Vision and Pattern Recognition (CVPR)*, pp. 1–9, Boston, MA, 2015.
- Bing Tian, Yong Zhang, Jin Wang, and Chunxiao Xing. Hierarchical Inter-Attention Network for Document Classification with Multi-Task Learning. In *Intl. Joint Conf. on Artificial Intelligence (IJCAI)*, pp. 3569–3575, 2019.
- Paul Voigtlaender, Patrick Doetsch, Simon Wiesler, Ralf Schlüter, and Hermann Ney. Sequence-Discriminative Training of Recurrent Neural Networks. In *Intl. Conf. on Acoustics, Speech, and Signal Processing (ICASSP)*, Brisbane, Australia, April 2015.
- Paul Voigtlaender, Patrick Doetsch, and Hermann Ney. Handwriting Recognition with Large Multidimensional Long Short-Term Memory Recurrent Neural Networks. In *Intl. Conf. on Frontiers in Handwriting Recognition (ICFHR)*, pp. 228–233, October 2016.
- Tianwei Wang, Yuanzhi Zhu, Lianwen Jin, Canjie Luo, Xiaoxue Chen, Yaqiang Wu, Qianying Wang, and Mingxiang Cai. Decoupled Attention Network for Text Recognition. In *Association for the Advancement of Artificial Intelligence (AAAI)*, volume 34(7), pp. 12216–12224, April 2020.
- Zhiguang Wang and Tim Oates. Imaging Time-Series to Improve Classification and Imputation. In *Intl. Joint. Conf. on Artificial Intelligence (IJCAI)*, pp. 3939–3945, Buenos Aires, Argentinia, July 2015.
- Curtis Wigington, Chris Tensmeyer, Brian Davis, William Barrett, Brian Price, and Scott Cohen. Start, Follow, Read: End-to-End Full-Page Handwriting Recognition. In *Euroop. Conf. on Computer Vision (ECCV)*, pp. 372–388, October 2018.
- Yijung Xiao and Kyunghyun Cho. Efficient Character-level Document Classification by Combining Convolution and Recurrent Layers. In *arXiv preprint arXiv:1602.00367*, February 2016.
- Mohamed Yousef and Tom E. Bishop. OrigamiNet: Weakly-Supervised, Segmentation-Free, One-Step, Full Page Text Recognition by Learning to Unfold. In *Intl. Conf. on Computer Vision and Pattern Recognition (CVPR)*, pp. 14710–14719, Seattle, WA, June 2020.
- Mohamed Yousef, Khaled F. Hussain, and Usama S. Mohammed. Accurate, Data-Efficient, Unconstrained Text Recognition with Convolutional Neural Networks. In *arXiv preprint arXiv:1812.11894*, December 2018.